

1 Article

# 2 Effect of configuration of a bulky aluminum initiator 3 on the structure of copolymers of *L,L*-lactide with 4 symmetric comonomer trimethylene carbonate

5 Marta Socka,\*Ryszard Szymanski,\*Stanislaw Sosnowski, and Andrzej Duda†

6 Centre of Molecular and Macromolecular Studies, Polish Academy of Sciences, 90-363 Lodz, Sienkiewiczza  
7 112, Poland; stasosno@cbmm.lodz.pl (S.S)

8 \* Correspondence: msocka@cbmm.lodz.pl (M.S.); rszymans@cbmm.lodz.pl (R.S); Tel.: +48-42-680-3314

9 † Deceased

10 **Abstract:** The effect of configuration of an asymmetric bulky initiator 2,2'-[1,1'-binaphtyl-2,2'-diyl-  
11 bis-(nitrylomethylidene)]diphenoxy aluminum isopropoxide (**Ini**) on structure of copolymer of  
12 asymmetric monomer *L,L*-lactide (**Lac**) with symmetric comonomer trimethylene carbonate (**Tmc**)  
13 was studied using polarimetry, dilatometry, SEC and <sup>13</sup>C NMR. When the *S*-enantiomer of **Ini** was  
14 used the distribution in copolymer chains at the beginning of polymerization is statistical, with  
15 alternacy tendency, changing next through a gradient region to homoblocks of **Tmc**. When,  
16 however, *R*-**Ini** was used, the product formed was a gradient oligoblock one, with **Tmc** blocks  
17 prevailing at the beginning, changing to **Lac** blocks dominating at end part of chains. Initiation of  
18 copolymerization with the mixture of both initiator enantiomers (*S*:*R* = 6:94) gave multiblock  
19 copolymer, of similar features but shorter blocks. Analysis of copolymerization progress required  
20 complex analysis of dilatometric data, assuming different molar volume contraction coefficients for  
21 units located in different triads. Comonomer reactivity ratios of studied copolymerizations were  
22 determined.

23 **Keywords:** Biodegradable copolyesters, copolymerization kinetics, copolymer microstructure,  
24 simulation, reactivity ratios, dilatometry  
25

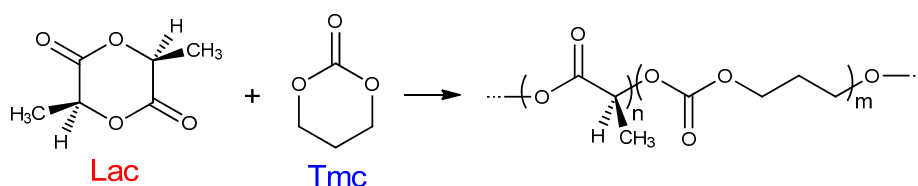
## 26 1. Introduction

27 Synthetic biodegradable polymers, *e.g.* aliphatic polyesters and polycarbonates as well as  
28 copolymers of the corresponding monomers, attract increasing attention because of their useful  
29 properties for applications in medical field as materials for temporary medical devices, such as  
30 scaffolds in tissue engineering or tissue reconstruction and drug-controlled-delivery systems [1,2].

31 Particularly, high modulus and high strength polylactides (PLac) have received special interest,  
32 as lactide (**Lac**) derives from annually renewable resources (*i.e.* corn starch or sugarcane). To the  
33 currently available products obtained from PLac belong sutures, GTR (guided tissue regeneration),  
34 orthopedic implants and implantable drug delivery systems [3-5].

35 However, due to PLac brittleness and relatively low resistance to oxygen and water vapor  
36 permeation, the range of possible applications of polylactides is restricted. Those properties could be  
37 altered by incorporation of different, suitable comonomer units into the main chain of PLac.

38 Copolymers containing lactide and carbonate units (*e.g.* trimethylene carbonate (**Tmc**), Scheme  
39 1):



40  
41 **Scheme 1.** Copolymerization of **Lac** and **Tmc**.

42 are especially interesting due to their increased flexibility and reduced acidity of the degradation  
43 products [6].

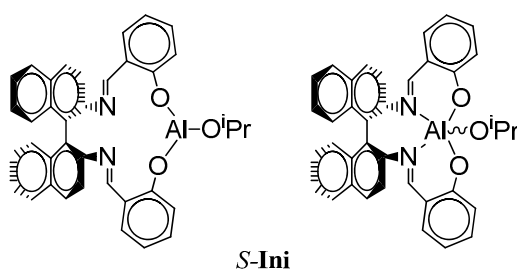
44 A ring-opening (co)polymerization (ROP) of aliphatic cyclic esters and carbonates is known as  
45 the most convenient method for the controlled synthesis of biodegradable and biocompatible  
46 copolymers [7]. Systematic studies on homopolymerization of lactones, lactides, and cyclic  
47 carbonates allowed to establish the fundamental thermodynamic, kinetic, and stereochemical  
48 aspects of these processes [7-10]. Particularly, controlled coordination polymerization of lactones  
49 and lactides that allowed preparation of polyester from oligomers to high molar mass polymers  
50 ( $M_n \sim 10^6$ ) with desired end groups, have been elaborated in our group [11].

51 In preparation of **Tmc/Lac** copolymers the tin derivatives are the most widely used  
52 catalyst/initiator systems [12-18]. The valuable results have also been obtained with various  
53 aluminum [19], lanthanide [20-22], and zirconium complexes [23]. The homopolymerization rates of  
54 **Tmc** and **Lac** are substantially different. Previous studies with the yttrium [24] and calcium [25]  
55 complexes proved that the rate of polymerization of **Tmc** is much higher than that for **Lac**.  
56 Nevertheless, during copolymerization of **Tmc** and **Lac**, both comonomers possess nearly the same  
57 reactivity ratio or the lactide monomer reveals higher reactivity. For example Yasuda *et al.* [26] have  
58 reported the formation of random **Tmc/Lac** copolymers in which both monomers exhibited similar  
59 reactivity ratios, using  $\text{SmMe}(\text{C}_5\text{Me}_5)_2\text{THF}$  initiator.

60 On the other hand, Spassky *et al.* [24] have reported the formation of almost pure block  
61 structure, in process initiated with yttrium alkoxide. The copolymerization of equimolar mixture of  
62 **Lac** and **Tmc** leads to the formation of block copolymers. **Lac** was consumed first due to its  
63 significantly higher reactivity ratio. Similarly, the reactivity ratios reported by Dobrzynski [23] ( $r_{\text{Lac}} =$   
64  $13.0$  and  $r_{\text{Tmc}} = 0.53$ ) proved favorable incorporation of repeating units derived from **Lac** into the  
65 copolymer chain. The product  $r_{\text{Lac}} \times r_{\text{Tmc}} = 6.89$  determined for the copolymerization initiated with  
66 zirconium complex was significantly higher than that previously reported for copolymerizations  
67 initiated with samarium complex [22] ( $r_{\text{Lac}} \times r_{\text{Tmc}} = 1.81$ ,  $r_{\text{Lac}} = 7.24$  and  $r_{\text{Tmc}} = 0.25$ ), and it was the  
68 evidence for a strong tendency to form a copolymer with a block structure.

69 The observed reactivities of **Tmc** and **Lac** in the copolymerization are reversed in comparison  
70 with their reactivities in homopolymerization, where the observed rates of polymerization of **Tmc**  
71 are higher than of **Lac** while applying the same initiator. Although the first report describing this  
72 puzzling phenomenon appeared about twenty years ago [24], to this day there is no plausible  
73 explanation on the molecular level.

74



75

76 **Scheme 2.** Structure of **S-Ini**. **R-Ini** enantiomer differs with conformation of binaphthyl residue,  
77 restricted due to inhibited rotation. Although the pentacoordinated structure is probably dominating  
78 in the reaction medium, we, for the sake of simplification, use tricoordinated structures in our other  
79 schemes.

80 The present work shows the preliminary results of our investigation of the effect of  
81 configuration of a bulky asymmetric initiator 2,2'-[1,1'-binaphthyl-2,2'-diyl-bis-(nitrylomethylidene)]-  
82 diphenoxy aluminum isopropoxide (**Ini**) (Scheme 2) on copolymerization of **Lac** with **Tmc**.

83 We have chosen this initiator because of its bulkiness, hindering chain transfer reactions and  
84 cyclization [27]. This feature was recently used by us in preparation of block **Lac/Tmc** copolymer by  
85 sequential copolymerization using this initiator [28].

86 The other reason of choosing the indicated initiator is its asymmetry resulting in asymmetry of  
 87 active chain-ends [29-31]. This feature implies possible differences in rates of addition of asymmetric  
 88 comonomer **Lac** in relation to configuration of active species of growing chain (configuration of  
 89 residue coming from *R* or *S*-**Ini**). These differences in propagation rate constants result in differences  
 90 of copolymer structure as shown in the paper.

91 Due to complexity of the systems discussed in the paper, the reported reactivity ratios are only  
 92 estimates, depending on the assumed model of copolymerization. They are, however, still useful in  
 93 predicting of the outcome of **Tmc/Lac** copolymerization in dependence on initial conditions.

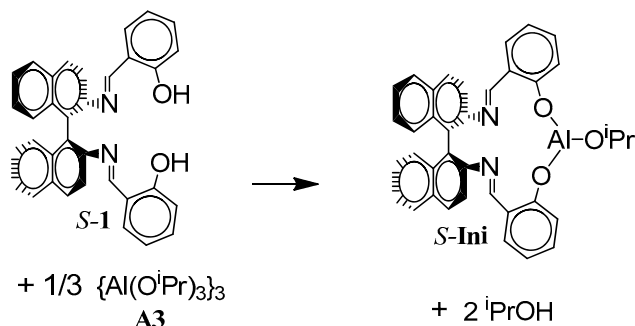
## 94 2. Materials and Methods

### 95 2.1. Materials

96 *L,L*-**Lac** (Boehringer Ingelheim, Germany, >99%) was crystallized from dry 2-propanol and then  
 97 purified by sublimation in vacuum ( $10^{-3}$  mbar, 90 °C). **Tmc** (Boehringer Ingelheim, Germany, >99%)  
 98 was crystallized from dry THF/ethyl ether mixture (3/1) and sublimed ( $10^{-3}$  mbar, 45 °C). THF  
 99 solvent was purified, as described previously [11]. Aluminum *tris*-isopropoxide used in trimeric  
 100 form  $\{Al(O^iPr)_3\}_3$  (**A3**) was prepared from the commercial alkoxide (Aldrich, 98%) as described  
 101 elsewhere [32,33]. Bidentate initiator precursor, asymmetric Schiff's base derivative, (*R*)-(-) and  
 102 (*S*)-(+)-2,2'-[1,1'-binaphthyl-2,2'-diyl-bis-(nitryl-methylidene)]diphenol (**1**), was prepared as described  
 103 in ref. 34.

### 104 2.2. Polymerization procedure

105 All polymerization were performed using the standard high-vacuum technique. The actual  
 106 initiator, *R*- and/or *S*-**Ini**, was formed *in situ* using **1** and **A3** in 1.2:1 ratio. The mixture was kept for  
 107 24 h in THF as a solvent at 80 °C just before use to ensure complete transformation of precursors to  
 108 **Ini**.



109

110

Scheme 3. *In situ* synthesis of *S*-**Ini**. Similarly *R*-**Ini** was formed.

111 The 20% excess of **1** did not affect the course of polymerization, both kinetics nor product  
 112 structure. The mixtures of comonomers and initiator in THF were prepared at room temperature in  
 113 the special glass vessels in a vacuum. Then the reaction mixture was distributed into several small  
 114 glass ampoules and/or into a dilatometer, and placed in thermostat at 80 °C. Both homo- and  
 115 copolymerization experiments have shown that isopropanol present in the initiating mixture acted  
 116 as effective chain-transfer agent. The observed number average molar masses  $M_n$  were  
 117 approximately equal as expected for all  $^iPrO$ - groups initiating chain growth,  $M_n =$   
 118  $(M_{Tmc}[Tmc]_0 + M_{Lac}[Lac]_0) / (3[Al(O^iPr)_3]_0)$  ( $M_{Tmc} = 102$  and  $M_{Lac} = 144$  are molar masses of corresponding  
 119 monomers). On the other hand, the dispersities observed for homopolymers were only slightly  
 120 higher than expected for processes without side reactions (about 1.1-1.2) and those observed for  
 121 copolymers were significantly higher (about 1.5-1.6), indicating probably not very fast rate of  
 122 exchange of chains bearing different terminal units at aluminum active centers (see discussion of  
 123 results).

124 Homopolymerizations of **Tmc** and **Lac** were used as reference in kinetic analysis, including  
125 molar volume contraction coefficients (CC) for dilatometry. Homopolymerization of monomers  
126 were carried out in THF at 80 °C with (S)-(-) and  
127 (R)-(+)-2,2'-[1,1'-binaphthyl-2,2'-diyl-bis-(nitrilomethylidyne)]diphenoxy aluminum isopropoxide  
128 (**Ini**). The starting concentrations of components were as follows:  
129  $[\text{Lac}]_0 = 1.2 \text{ mol L}^{-1}$ ,  $[\text{Tmc}]_0 = 2 \text{ mol L}^{-1}$  and  $[\text{Ini}]_0 \approx 0.002 \text{ mol L}^{-1}$ . The conversion of **Lac** in both homo-  
130 and copolymerizations was monitored by polarimetry while conversion of **Tmc** in  
131 homopolymerizations was monitored with dilatometry and in copolymerizations it was determined  
132 at various reaction times from a complex analysis of copolymerization kinetics, consistent with  
133 kinetics of changes of dilatometer meniscus level, as described below.

134 The resulting (co)polymers were isolated by precipitation into cold methanol, and dried in  
135 vacuum at room temperature to a constant mass. For comparative studies two poly(trimethylene  
136 carbonate) (PTmc) and two poly(L-lactide) (PLac) homopolymers, *i.e.*, PTmcs with  $M_n$  of  $33.8 \cdot 10^3$  and  
137  $32.1 \cdot 10^3$  ( $D \approx 1.5$ ) as well as PLacs with  $M_n$  equal to  $23.5 \cdot 10^3$  and  $22.2 \cdot 10^3$  ( $D = 1.4$  and  $1.8$  respectively),  
138 have been prepared.

139 Copolymers of **Lac** and **Tmc** were obtained in ring-opening copolymerization, initiated with  
140 (S)-(-)-**Ini** or (R)-(+)-**Ini**, or with the chosen mixture of both initiator enantiomers, at 80 °C in THF. All  
141 experiments were carried out with identical initial concentrations of **Tmc** and initiator:  $[\text{Tmc}]_0 = 2$   
142  $\text{mol L}^{-1}$  and  $[\text{Ini}]_0 = 0.002 \text{ mol L}^{-1}$  (prepared *in situ*, cf. Scheme 3: concentration of growing chains  
143 equal to  $0.006 \text{ mol L}^{-1}$  due to initial presence of  $^i\text{PrOH}$ , acting as an effective chain transfer agent).  
144 Concentration of  $[\text{Lac}]_0$  varied from 0.3 to  $1.2 \text{ mol L}^{-1}$ .

### 145 2.3. Carbon Nuclear Magnetic Resonance ( $^{13}\text{C}$ NMR)

146 Composition and microstructure of copolymers were determined by NMR spectroscopy.  $^{13}\text{C}$   
147 NMR spectra were recorded on a Bruker AVANCE III (apparatus operating at 500 MHz) in  $\text{CDCl}_3$   
148 (99.8% D) as the solvent. The sample solutions were prepared by dissolving 15-30 mg of dried  
149 polymer in 1 mL of  $\text{CDCl}_3$ .  $^{13}\text{C}$  NMR spectra were recorded with inverse gated decoupling, allowing  
150 one to minimize the errors of quantitative analyses.

### 151 2.4. Size Exclusion Chromatography (SEC)

152 The SEC chromatograph was composed of Agilent 1100 isocratic pump, MALLS DAWN EOS  
153 photometer (Wyatt Technology Corporation) and Optilab Rex differential refractometer (Wyatt  
154 Technology Corporation). Two PL Gel 5- $\mu\text{m}$  MIXD-C columns were used in a series for separation.  
155 Methylene chloride was used as a mobile phase at a flow rate of  $0.8 \text{ mL min}^{-1}$ . The measurements  
156 were conducted at 27 °C. The calibration of the DAWN EOS was performed using p.a. grade toluene,  
157 and normalization was performed using a polystyrene standard (PS:  $M_n = 3.0 \cdot 10^4$ , Polymer  
158 Standards Service). The ASTRA 4.90.07 software package (Wyatt Technology Corporation) was used  
159 for the data collection and processing.  $dn/dc$  increments of the refractive index were determined at  $\lambda$   
160  $= 658 \text{ nm}$ , as  $0.048$  and  $0.035 \text{ mL g}^{-1}$  for PTmc and PLac, respectively. Samples ( $100 \mu\text{L}$ ) were injected  
161 as solutions in methylene chloride.  
162

### 163 2.5. Polarimetry

164 A Perkin-Elmer 241 MC polarimeter was employed for the optical rotation measurements. The  
165 optical rotations (OR) of the living polymerization mixtures were measured at 578 nm at room  
166 temperature. The instantaneous **Lac** concentrations were determined, assuming additivity of the  
167 optical rotations for **Lac** ( $\text{ORM} = 270^\circ$ ) and poly-**Lac** ( $\text{ORP} = 166^\circ$ ), *i.e.*,  
168  $[\text{LA}] = [\text{LA}]_0 (\text{OR} - \text{ORP}) / (\text{ORM} - \text{ORP})$ .

169  
170

## 171 2.6. Dilatometry

172 (Co)polymerizations of **Tmc** were carried out in dilatometers equipped with capillary tubes.  
173 Dilatometers, of volume about 5 mL, precisely measured, were put in the thermostated water bath in  
174 order to perform accurate measurements of the volume changes during polymerization, calculated  
175 from measurements of the meniscus level in the capillary tube, diameter 2 mm, with accuracy 0.01  
176 mm. The instantaneous **Tmc** concentrations in polymerization were determined assuming additivity  
177 of the polymer and monomer density, using the corresponding equation:  $[\mathbf{Tmc}] = [\mathbf{Tmc}]_0 \Delta H / \Delta H_{\max}$ ,  
178 where  $\Delta H$  and  $\Delta H_{\max}$  are the changes of meniscus level at the given reaction time and when reaching  
179 total conversion of **Tmc**, respectively (small **Tmc** equilibrium concentration was neglected).

180 The attempts to determine in the same way consumption of **Tmc** in copolymerization failed  
181 because the molar volume-contraction-coefficients (CC) for **Tmc** units located in different triads  
182 appeared to be not equal. The elaborated method for determining **Tmc** consumption in  
183 copolymerization from dilatometric data, based on fitting of simulated copolymerization  
184 conversions to experimental ones, is described in details in Supporting information.

185

## 186 2.5. Computer simulations

187 Kinetics of studied copolymerizations were analyzed comparing experimental data with  
188 computer simulations carried out on personal computer with Intel Core i7-975 processor working at  
189 frequency 3.33 GHz, 12 GB RAM memory, under Microsoft Windows 7 Pro 64-bit operating system.

190 Two types of numerical computations were used. Numerical integrations of kinetic differential  
191 equations were performed in Matlab v. 7.10, adopting the Matlab function *ode15s*, while parameter  
192 fitting performed using the function *fminsearch*. For more details see the Supporting Information.  
193 The computational times of fitting kinetic parameter to experimental data varied between 2 to 48 h,  
194 depending on the number of fitted parameters. Monte-Carlo computations were performed using  
195 in-house prepared computation programs, according to algorithm devised by Gillespie [35].  
196 Programs were written in Delphi and compiled under Delphi XE2 environment (Embarcadero,  
197 USA). Times of simulations varied in a range of 2–48 h, depending on the number of simulated  
198 chains, selected kinetic parameters, and on accounting or neglecting of depropagation reactions

## 199 3. Results

200 In this work we determined that the relative reactivities of **Tmc** and **Lac** in the copolymerization  
201 differ considerably from their reactivities in homopolymerizations, similarly as it was observed for  
202  $\epsilon$ -caprolactone/**Lac** systems initiated with the same initiator **Ini** [32]. Significant discrepancies in  
203 reactivities of active centers differing in configuration of the used initiator were already observed in  
204 **Lac** homopolymerization studies [31]. It stems from different diastereomeric arrangements at the  
205 end of growing chains formed by asymmetric **Lac** terminal unit (*S* configuration) and residue from  
206 *R*- or *S*-**Ini**. Results of our reference **Lac** homopolymerizations, performed for  $[\mathbf{Lac}]_0 = 1.2 \text{ mol L}^{-1}$ , are  
207 shown in Supporting information, confirming large differences in rates of polymerization. On the  
208 other hand, one cannot expect any differences in **Tmc** homopolymerization rates, what was  
209 confirmed experimentally (initial rate coefficients equal to about 0.088 and 0.093 ( $\pm 5\%$ )  $\text{L mol}^{-1} \text{ s}^{-1}$ , for  
210 polymerizations initiated with *R*-**Ini** and *S*-**Ini**, respectively). Therefore, we could expect that the  
211 copolymerization reactivity ratios change by altering the active-center initiator-residue  
212 configuration, what can result in quite different copolymer structures. In fact, the differences in  
213 reactivity ratios were larger than expected by us.

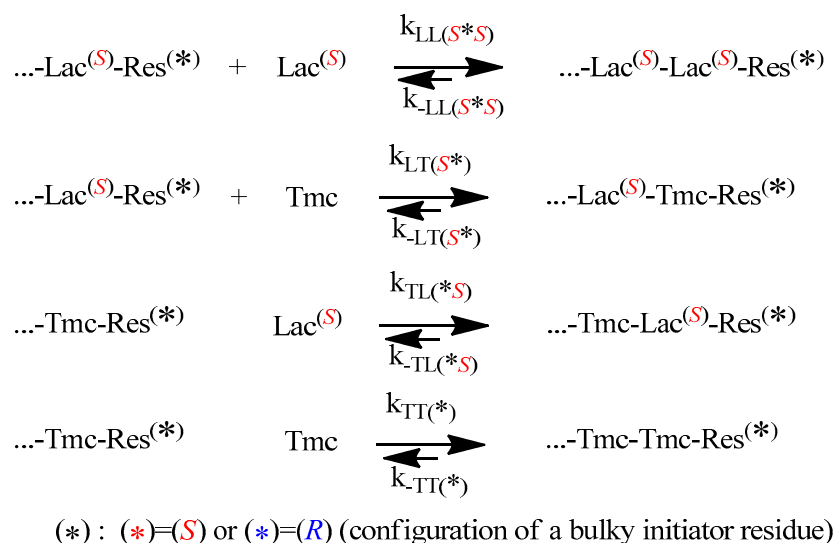
214 This striking phenomenon is of general importance, since it provides a useful tool for tuning the  
215 resultant copolymer microstructure and properties.

216

217

## 218 3.1. Outlook of general features of copolymerization kinetics

219 The propagation and depropagation reactions, describing the studied copolymerization, are  
 220 shown in Scheme 4.

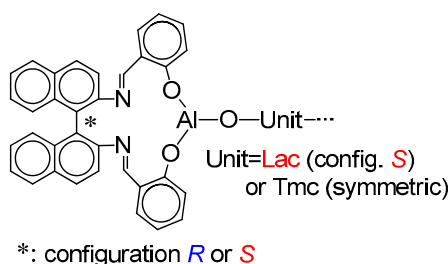


221

222 **Scheme 4.** Chemical reactions governing copolymerization of **Lac** with **Tmc** (M in the Scheme). 'Res'  
 223 denotes the asymmetric residue coming from initiator.

224 One can note that diastereomeric arrangements imply differences in propagation and  
 225 depropagation rate constants, in relation to configuration of used initiator, with the exception of the  
 226 last reversible reaction in the Scheme 4: homopropagation and corresponding depropagation of **Tmc**  
 227 (apparently no diastereometry, one can expect identical reactivity of enantiomeric **Tmc-Res\***).

228 The structure of active species is shown in Scheme 5. If the copolymer unit is symmetric (**Tmc**),  
 229 one can expect that the rate of insertion of alike monomer molecule into Al-O-Unit bond does not  
 230 depend on configuration of initiator residue **Res** at the chain-end. On the other hand, addition of  
 231 asymmetric monomer molecule (**Lac**) depends on configuration of **Res** because we can have two  
 232 different diastereomeric arrangements here. Similarly, when Unit is asymmetric (**Lac**), addition of  
 233 any of comonomers (**Lac** or **Tmc**) depends on configuration of **Res** (reactions involving  
 234 diastereomeric active species).



235

236 **Scheme 5.** Schematic presentation of the active chain-end in copolymerization of **Lac** with **Tmc**.

237 Thus, depending on configuration of **Ini**, copolymerization can proceed in a different way.

238 In principle, copolymerization kinetics can be monitored by any method giving access to  
 239 comonomer conversions. Unfortunately spectroscopic methods we considered (UV, IR, <sup>1</sup>H NMR)  
 240 could not be used effectively because of the lack of sufficiently separated signals of comonomers and  
 241 copolymer. Only <sup>13</sup>C NMR spectra could give the corresponding information. Unfortunately, due to  
 242 technical problems (taking samples from the reaction mixture avoiding its contamination, followed  
 243 by isolation of product) only a few kinetic data points could be obtained. Much more convenient  
 244 methods seemed polarimetry for following conversion of **Lac** and dilatometry for following  
 245 conversion of **Tmc** (polymerization of **Lac** results in no change of the reaction system volume),

246 following the approach, applied by Florczak and Duda in analysis of copolymerization kinetics of  
 247 **Lac** with  $\epsilon$ -caprolactone [32].

248 However, it appeared that following conversion of **Tmc** with dilatometry was not  
 249 straightforward. We have observed that changes of the system volume were significantly larger than  
 250 expected on the basis of contraction coefficients determined from homopolymerization of **Tmc**.  
 251 Moreover, conversion of **Tmc** determined from dilatometry in a standard way was significantly  
 252 different from that obtained from  $^{13}\text{C}$  NMR, available for a few reaction times of one  
 253 copolymerization system, initiated with the mixture of *R*- and *S*-**Ini** (cf. below in the corresponding  
 254 section).

255 Consequently, we came to conclusion that contraction coefficients for **Tmc** and, possibly, also  
 256 for **Lac** units, depend on the type of triad in which the given unit occupies the central place. Thus, in  
 257 order to be able of using dilatometry for following the **Tmc** conversion, we had to determine, or at  
 258 least estimate, three values of contraction coefficients for any of comonomers, e.g. for A unit  
 259 coefficients for homotriad AAA, heterotriad BAB, and the average value for asymmetric triads AAB  
 260 and BAA. The average value for asymmetric triads is sufficient because in copolymer of sufficiently  
 261 long chains the numbers of triads AAB and BAA are virtually equal.

262 However, in order to estimate these parameters directly we would have to have a sufficiently  
 263 large number of experimental data describing relation between comonomer conversions and  
 264 copolymer microstructure (triad level), and volume contraction corresponding to the given samples.

265 Unfortunately,  $^{13}\text{C}$  NMR did not give the sufficient information about triad (nor dyad)  
 266 contributions, because some triads, assigned according to Dobrzynski and Kasperczyk [23], overlap  
 267 (e.g. of triads **TmcLLTmc**, **LacLLTmc** and **TmcLLLac**: LL means here **Lac** unit, composed of two  
 268 lactic units L, in bold are marked the lactic units relevant to overlapping signals, cf. Table 1).  
 269

270 **Table 1.** Assignment of the resonance lines in the  $^{13}\text{C}$  NMR spectra of **Lac** (composed of 2 lactic units  
 271 denoted here as L: **Lac=LL**) and **Tmc** copolymer units in copolymers.

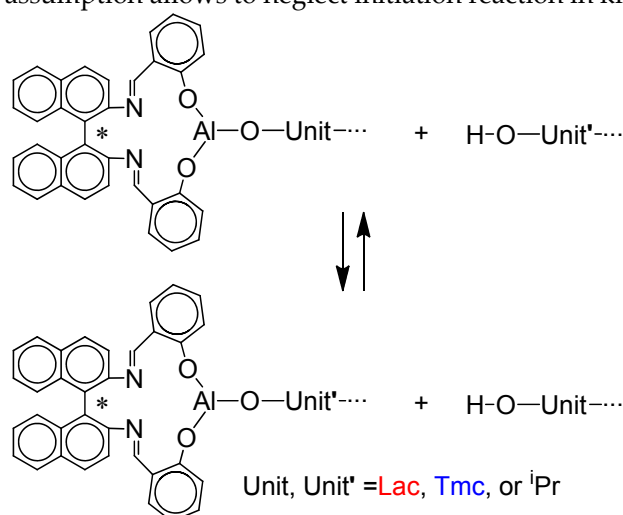
	Resonance line (i)	Comonomer sequence	$\delta$ (ppm) <sup>a</sup>
The carbonyl carbon atoms absorption range			
<b>Lac</b> repeating units (LL)	1	TLLT+ LLLLT + TLLLT	- (170.24)
	2	TLT	170.14 (170.09)
	3	TLLT + TLLLL + TLLLT + LLLLT	169.97 (169.92)
	4	TLLLT + TLLLL	169.79 (169.75)
	5	LLLLL	169.61 (169.57)
<b>Tmc</b> repeating units (T)	6	TTT + LLTT + TLTT	154.89 (154.85)
	7	TTLL + LLTLL + TLTLL	154.33 (154.29)
	8	TTLT + LLTLT + TLTLT	- (153.85)
The methine carbon atoms absorption range			
<b>Lac</b> repeating units (LL)	9	TLT	- (71.98)
	10	TLLLT	71.75 (71.71)
	11	TLLT	71.65 (71.60)
	12	TLLLT + TLLLT	71.38 (71.33)
	13	TLLLL+ LLLLT	69.26 (69.20)
	14	LLLLL	69.03 (68.98)
The methylene carbon atoms absorption range <sup>b</sup>			
<b>Tmc</b> repeating units (T)	15	LT'T + TT''L	64.74 (64.70)
	16	TT'T + TT''T	64.28 (64.24)
	17	LT'L + LT''L	- (61.79)
	18	TT'L + TT''T	61.70 (66.66)

272 <sup>a</sup> In parentheses data from ref. 23 are listed; <sup>b</sup> T' = -OCH<sub>2</sub>CH<sub>2</sub>CH<sub>2</sub>-OCO-, T'' = -OCH<sub>2</sub>CH<sub>2</sub>CH<sub>2</sub>-OCO-

273 Signals of copolymer structures stemming from segmental exchange (e.g. of the isolated lactic  
274 unit TmcLTmc) were observed by us only in spectra of system kept more than 24 h after completing  
275 copolymerization what confirms our assumption that reshuffling can be neglected.

276 We managed to estimate the contraction coefficients from analysis of copolymerization kinetics.  
277 Unfortunately, some assumptions, leading eventually to estimates valid only for the assumed model  
278 of copolymerization, had to be adopted. These assumptions were as follows:

- 279 1. Kinetics of copolymerization follows the reactions as reported in Scheme 4 and  
280 depolymerizations can be neglected up to at least 80% of conversion. The last is based on our  
281 simulations of reversible copolymerizations [36], indicating that depolymerizations with  
282 low equilibrium concentrations of comonomers are usually negligible in most systems up to  
283 conversions about 90%.
- 284 2. The chain-transfer reactions involving hydroxyl containing chains are fast, allowing to  
285 neglect them in kinetic analysis and consider all chains terminated with the given unit  
286 kinetically indistinguishable. Alcohol chain end-groups in the copolymerization systems are  
287 formed at the very beginning of copolymerization due to the fact that we initiated our  
288 systems with the *in situ* formed **Ini** (Scheme 3), what resulted in formation of isopropanol,  
289 which also can initiate copolymer chains via chain-transfer processes (Scheme 6). The  
290 chain-transfer reactions were, however, taken into account in more detailed kinetic analysis,  
291 allowing to get better agreement of experimental and simulated dispersities of copolymers.
- 292 3. Instantaneous initiation gives living unimers prior to any propagation reactions. This  
293 approximating assumption allows to neglect initiation reaction in kinetic analysis.



294

295 **Scheme 6.** Chain-transfer reactions operating in the studied copolymerization systems. Due to the  
296 assumption of instantaneous initiation isopropyl (iPr) containing active species, as well as iPrOH,  
297 coming from the *in situ* synthesis of **Ini** (cf. Scheme 3), could be neglected.

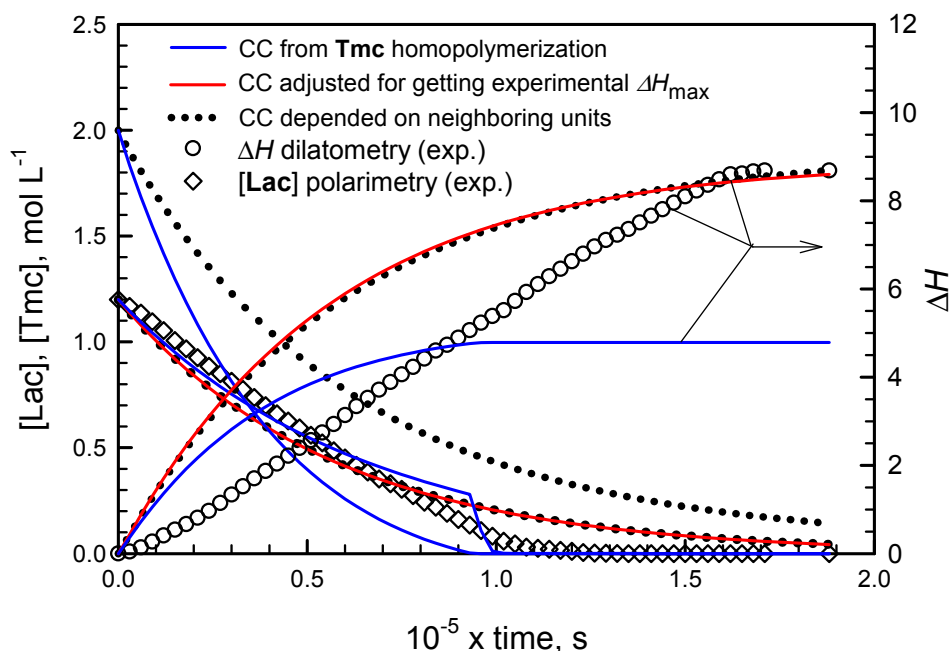
298 These assumptions allowed us to describe copolymerization systems entirely by the kinetic  
299 Scheme 4, not accounting OH-terminated chains. Such a simple model of copolymerization  
300 appeared to be useful if copolymerization main features, such as copolymer composition and  
301 microstructure, are concerned. When, however, more detailed features, like molar mass distribution  
302 are to be analyzed, the copolymerization model including the rate of exchange of OH-terminated  
303 chains with ones bearing active species, has to be used, as shown below in the paper.

304 Nevertheless, kinetics of irreversible copolymerizations following Scheme 4 (with all  
305 depropagation rate constant equal to zero) can be predicted from integration of the corresponding  
306 kinetic differential equations. On the other hand, Monte Carlo simulations, taking into account  
307 depropagations, could confirm validity of neglecting them, as well as could give access to detailed  
308 description of copolymer microstructure.

309 Applying numerical integration of differential kinetic equations we could predict evolution of  
310 copolymerization in time. However, attempts to fit rate coefficients failed, indicating that



311 comonomer consumption rates seemed not to decrease with comonomer concentrations as expected.  
 312 Rates of consumption of comonomers were initially lower than those predicted from simulations  
 313 and eventually higher: the apparent rate coefficients seemed to increase with conversion. An  
 314 example of such fitting is given in Figure 1. More details concerning this type of kinetic analysis are  
 315 given in Supporting information.  
 316



317

318 **Figure 1.** Fitting of simulated changes of  $[\text{Lac}]$  (lines starting from  $[\text{Lac}] = 1.2$ ) and of the dilatometer  
 319 meniscus height  $\Delta H$  (lines starting from  $\Delta H = 0$ ) to experimental data (diamonds:  $[\text{Lac}]$ , circles:  
 320 meniscus  $\Delta H$ ) for copolymerization of **Lac** with **Tmc**, initiated with  $[\text{S-Ini}] = 2 \cdot 10^{-3}$  ( $[\text{PrOH}]_0 = 4 \cdot 10^{-3}$   
 321  $\text{mol L}^{-1}$  due to *in situ* synthesis of **Ini**),  $[\text{Lac}]_0 = 1.2$ ,  $[\text{Tmc}]_0 = 2 \text{ mol L}^{-1}$ . Blue lines: volume contraction  
 322 coefficient (CC) for **Tmc** copolymerization equal to that determined from homopolymerization  
 323 experiments, red lines: CC for **Tmc** units increased to get the same final meniscus height as  
 324 determined experimentally, black dot lines: **Tmc** and **Lac** unit CC depending on neighboring units,  
 325 as determined in our studies (see Supporting information). Additionally the predicted changes of  
 326  $[\text{Tmc}]$  are presented (lines starting from  $[\text{Tmc}] = 2$ ).

327 The presented plots suggest that apparent rate coefficients change with conversion, being  
 328 initially lower than obtained from parameter fitting (experimental slope for evolution of  $[\text{Lac}]$   
 329 initially lower than obtained in simulations) and, at the end of comonomer consumption, the rate  
 330 coefficients seem to be higher than obtained from simulations (the corresponding slope for  
 331 experimental points for reaction times longer than 1000 min is higher than that of fitted plots).

332 Important is also observation that volume contraction coefficients for copolymer units differ  
 333 from those observed in homopolymerizations. Either contraction coefficients for **Tmc** unit depend  
 334 on other units neighboring the given one, or the same can be said about **Lac** units (contraction  
 335 coefficients for some triads with **Lac** located in the middle not equal to zero as in  
 336 homopolymerization), or contraction coefficients for both types of copolymer units depend on  
 337 copolymer microstructure. Our fitting analysis (see below and Supporting information) suggest that  
 338 the third possibility is true.

339 Analyzing simulated kinetic curves in comparison to experimental ones we deduced that the  
 340 reaction medium, continuously changing while concentrations of comonomers and copolymer units  
 341 evolve, makes the rate coefficients depending on conversion. It can be understood as both  
 342 comonomer molecules and copolymer units solvate active species in varying proportions at different

343 conversions. As **Lac** molecule and copolymer units are asymmetric one cannot exclude some  
344 diastereomeric effect making the apparent rate coefficients dependent on conversion.

345 In order to get a relatively simple kinetic model of copolymerization consistent with  
346 experimental data we have assumed that the relative changes of apparent rate coefficients with  
347 conversion are approximately identical for all reactions, changing simultaneously, resulting in  
348 constant ratios of rate constants. The analyzed models of copolymerization and methods of fitting  
349 apparent relative rate coefficients to experimental data are described in detail in Supporting  
350 information. Here we only indicate the main result of this analysis. Namely, if the abovementioned  
351 assumption is valid then the kinetics presented in conversion scale is characterized by kinetic  
352 parameters independent of conversion or reaction time. These kinetic parameters are ratios of  
353 instantaneous (changing) rate coefficients of reactions operating in the system. One can choose  
354 different ratios to describe the analyzed copolymerizations but our choice was as given below.

355 Initially, we related all rate constants to the **Tmc** homopropagation rate constant  $k_{TT}$  (see  
356 Scheme 4), chosen as the rate constant presumably independent of configuration of **Ini** and denoted  
357 the corresponding ratios  $z_{XY} = k_{XY}/k_{TT}$ , where X, Y is L and/or T, which stand for **Lac** or **Tmc**  
358 comonomer/unit.

359 However, one can easily find that one can relate these  $z_{XY}$  parameters (XY different than LL)  
360 with  $z_{LL}$  and standard parameters such as reactivity ratios and, for depropagation rate constants,  
361 additionally with the equilibrium constants. These relationships are presented in the equation set (1).  
362 Starting from this equation set we use letters L and T, while denoting with **Lac** and **Tmc**  
363 comonomers/comonomer units, respectively. Besides, in all equation sets we use for these letters red  
364 and blue color, respectively. The same colors are used in some Figures and plots describing  
365 copolymer units or blocks related to the studied comonomers.

$$\begin{aligned}
 z_{LL} &= \frac{k_{LL}}{k_{TT}}, \quad z_{TT} = \frac{k_{TT}}{k_{TT}} = 1 \\
 z_{LT} &= \frac{k_{LT}}{k_{TT}} = \frac{k_{LT}}{k_{LL}} \times \frac{k_{LL}}{k_{TT}} = \frac{z_{LL}}{r_L}, \quad z_{TL} = \frac{k_{TL}}{k_{TT}} = \frac{1}{r_T} \\
 z_{-LL} &= \frac{k_{-LL}}{k_{TT}} = \frac{k_{-LL}}{k_{LL}} \times \frac{k_{LL}}{k_{TT}} = \frac{z_{LL}}{K_{LL}}, \quad z_{-TT} = \frac{k_{-TT}}{k_{TT}} = \frac{1}{K_{TT}} \\
 z_{-LT} &= \frac{k_{-LT}}{k_{TT}} = \frac{k_{-LT}}{k_{LT}} \times \frac{k_{LT}}{k_{LL}} \times \frac{k_{LL}}{k_{TT}} = \frac{z_{LL}}{K_{LT}r_L}, \quad z_{-TL} = \frac{k_{-TL}}{k_{TT}} = \frac{1}{K_{TL}r_T}
 \end{aligned}
 \tag{1}$$

367 Thus, we could formulate the kinetic differential equations in conversion scale, with only the  
368 limited number of the mentioned relative kinetic parameters:  $z_{LL}$  and reactivity ratios  $r_L$  and  $r_T$  (and  
369 for not negligible depropagations also the equilibrium constants), taking into account the following  
370 relationships (formulated here for irreversible copolymerization):

$$\begin{aligned}
 Conv &= \int_0^t \left( \frac{-d[L]}{dt} - \frac{d[T]}{dt} \right) dt \\
 \frac{dConv}{dt} &= \frac{\left( -\frac{d[L]}{dt} - \frac{d[T]}{dt} \right)}{[L]_0 + [T]_0} = \frac{k_{LL}[L^*][L] + k_{TL}[T^*][L] + k_{TT}[T^*][T] + k_{LT}[L^*][T]}{[L]_0 + [T]_0} \\
 \frac{d[ ]}{dConv} &= \frac{\frac{d[ ]}{dt}}{\frac{dConv}{dt}} = f([L], [T], \dots, z_{LL}, r_L, r_T)
 \end{aligned}
 \tag{2}$$

372 where [ ] in the equation (2) corresponds to concentration of any reagent, species, or copolymer  
373 sequence in copolymer. For instance, the corresponding equations formulated for evolution of  
374 concentrations of **Lac** (L) monomer and LT dyads are given by equation set (3):

375

$$\frac{d[L]}{dConv} = -([L]_0 + [T]_0) \times \frac{z_{LL}[L^*][L] + [T^*][L]/r_T}{z_{LL}[L^*][L] + [T^*][L]/r_T + [T^*][T] + z_{LL}[L^*][T]/r_L} \quad (3)$$

$$\frac{d[T]}{dConv} = ([L]_0 + [T]_0) \times \frac{z_{LL}[L^*][T]/r_L}{z_{LL}[L^*][L] + [T^*][L]/r_T + [T^*][T] + z_{LL}[L^*][T]/r_L}$$

377

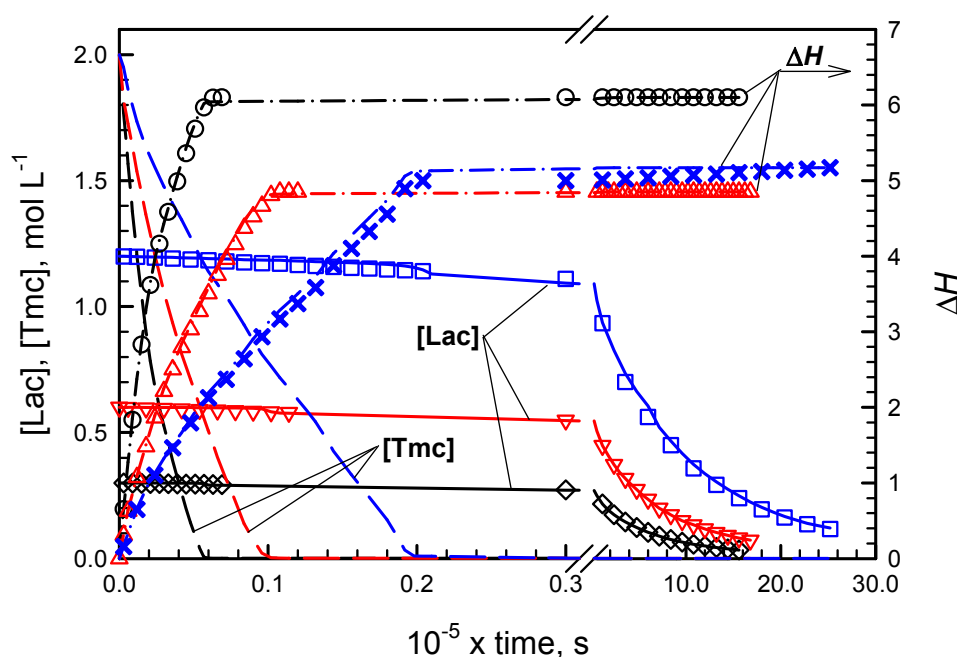
378 Applying the formulated set of kinetic differential equations in conversion scale (see  
 379 Supporting information) to experimental data allowed us to predict main features of copolymers  
 380 obtained in the studied systems.

### 381 3.2. Dependence of copolymer structure on configuration of *Ini*

382 Figures 2 and 3 present conversions of comonomers in copolymerizations initiated with *R*- and  
 383 *S*-*Ini*, respectively. Conversions of **Lac** were detected directly due to polarimetric measurements  
 384 while conversions of **Tmc** were obtained from the elaborated kinetic analysis presented in  
 385 Supporting information. The kinetic and contraction parameters were fitted to describe  
 386 simultaneously three copolymerization experiments initiated with the given enantiomer of *Ini*,  
 387 differing with the initial **Lac** concentrations.

388

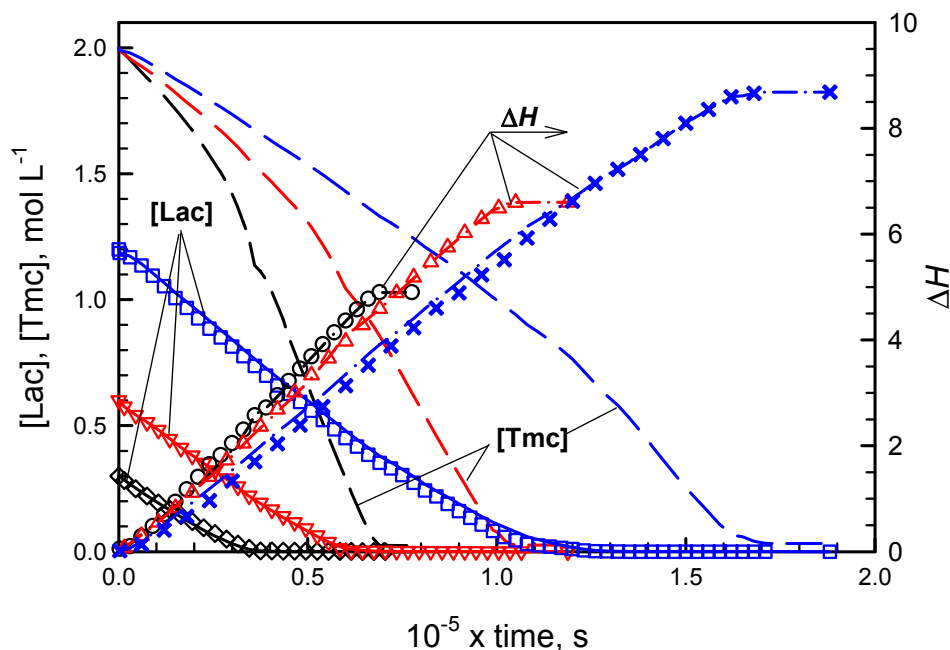
389



390

391 **Figure 2.** Experimental and simulated evolution of **[Lac]**, **[Tmc]**, and  $\Delta H$  in copolymerizations  
 392 initiated with *R*-*Ini* for different **[Lac]**<sub>0</sub>: 0.3 (black), 0.6 (red), and 1.2 mol L<sup>-1</sup> (blue). Experimental data  
 393 marked by symbols, simulated data by lines. Other initial conditions: **[Tmc]**<sub>0</sub> = 2 mol L<sup>-1</sup>. **[R-Ini]**<sub>0</sub> = 2  
 394 10<sup>-3</sup> mol L<sup>-1</sup> (+ **[iPrOH]**<sub>0</sub> = 4 10<sup>-3</sup> mol L<sup>-1</sup> due to *in situ* synthesis of *Ini*).

395



396

397

398

399

**Figure 3.** Experimental and simulated evolution of [Lac], [Tmc], and  $\Delta H$  in copolymerizations initiated with *S-Ini*. Plots description and copolymerization conditions as given in caption for Figure 2, but *R-Ini* enantiomer was used.

400

401

402

403

404

405

406

While in systems with *R* initiator enantiomer, initially mostly **Tmc** is consumed, giving presumably the product resembling diblock copolymer, in systems with *S-Ini* we obtained product containing in the initial parts of chains both comonomers in similar quantities. The chains are terminated eventually with **Tmc** blocks due to the fact that **Lac** was consumed before **Tmc**, used in significant excess. Kinetic analysis confirms this description of products giving both reactivity ratios much higher than unity in *R-Ini* systems and the product of reactivity ratios lower than unity in *S-Ini* systems.

407

408

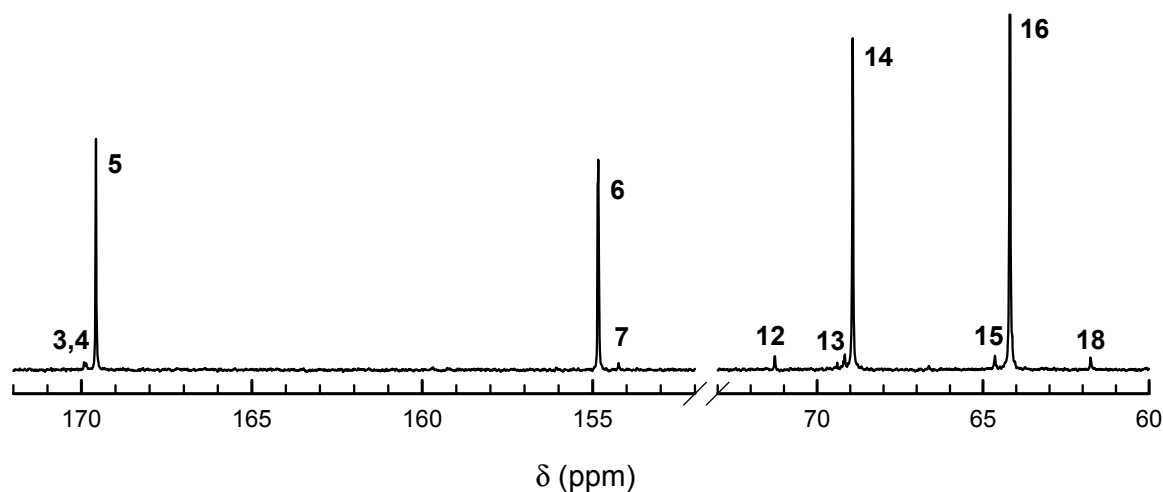
409

410

411

412

$^{13}\text{C}$  NMR spectra (Figure 4 and 5) also confirm the above description of copolymers, indicating the large excess of homodyads in products initiated with *R-Ini* and a low quantity of homodyads LacLac in copolymer initiated with *S-Ini*, what indicates some tendency to alternacy, as expected from the estimated product of reactivity ratios being significantly lower than unity. Assignment of  $^{13}\text{C}$  NMR signals is given in Table 1.



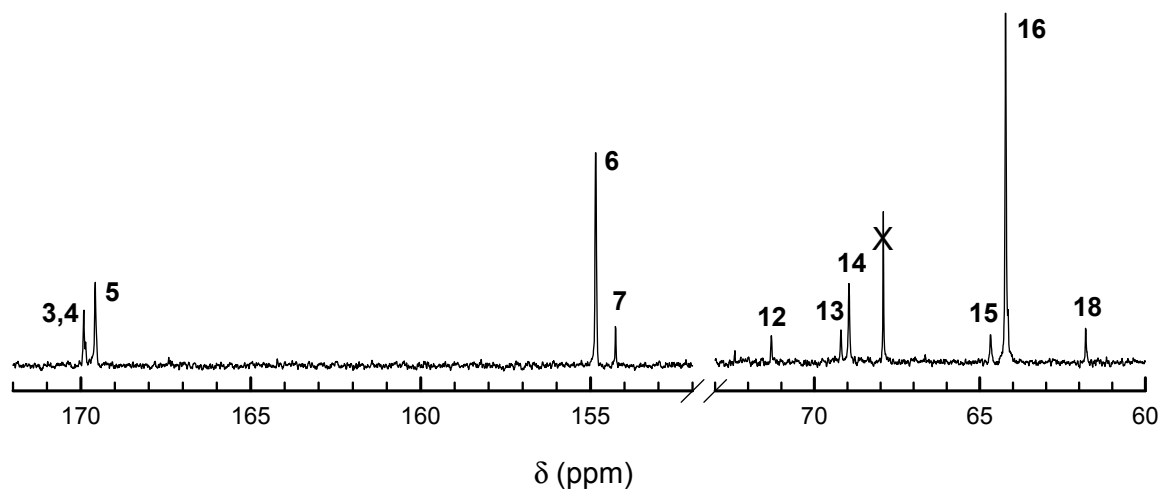
413

414

415

**Figure 4.**  $^{13}\text{C}$  NMR spectra of **Tmc/Lac** copolymers prepared with *R-Ini*. Polymerization conditions:  $[\text{Lac}]_0$ ,  $[\text{Tmc}]_0$ ,  $[\text{R-Ini}]_0 = 1.2, 2, \text{ and } 2 \cdot 10^{-3}$  ( $+ [\text{PrOH}]_0 = 4 \cdot 10^{-3}$ )  $\text{mol L}^{-1}$ , respectively. Time  $3.81 \times 10^6 \text{ s}$ ,

416 conversion **Lac** = 92%, conversion **Tmc** = 99%. Note large contributions of signals of homo **Lac** and  
417 **Tmc** sequences, signals 13, and 15, respectively. Assignment of signals is given in Table 1.



418  
419 **Figure 5.**  $^{13}\text{C}$  NMR spectra of **Tmc/Lac** copolymers prepared with *S*-**Ini**. Polymerization conditions:  
420  $[\text{Lac}]_0$ ,  $[\text{Tmc}]_0$ ,  $[\text{S-Ini}]_0 = 1.2, 2, \text{ and } 2 \cdot 10^{-3}$  ( $[\text{iPrOH}]_0 = 4 \cdot 10^{-3}$ ) mol L $^{-1}$ , respectively. Time  $1.49 \times 10^5$  s,  
421 conversion **Lac** = 96%, conversion **Tmc** = 99%. Note a relatively low contribution of a signal of homo  
422 **Lac** sequences (signal 13), and quite large contribution of **TmcLacTmc** sequence (signal 10).  
423 Assignment of signals is given in Table 1.

424 Our kinetic analysis allowing us to estimate the reactivity ratios for the studied systems is  
425 described in details in Supporting information. It was based on fitting of the simulated evolution of  
426 the studied systems, described by the formulated differential kinetic equations with the relative  
427 kinetic parameters, including reactivity ratios, to experimental evolution of the studied systems.

428 Main results of the primary kinetic analysis are given in Table 2 while the Figures 2 and 3  
429 present experimental and computed from kinetic analysis evolution of copolymerizations initiated  
430 with *R* and *S* enantiomers of **Ini**.

431 **Table 2.** The reactivity ratios and relative rates of comonomer consumption<sup>a)</sup> estimated for **Lac/Tmc**  
432 copolymerization systems initiated with *R*-**Ini** and *S*-**Ini**.

Initiator	<i>R</i> - <b>Ini</b>	<i>S</i> - <b>Ini</b>
$r_L$	21.5	1.11
$r_T$	$2.5 \times 10^2$	$9.7 \times 10^{-2}$
$d[\text{Lac}]/d[\text{Tmc}]$	$4.1 \times 10^{-4}$ (0.05)	0.17 (0.02)
	<b><math>2.5 \times 10^{-3}</math> (0.15)</b>	0.36 (0.05)
	<b><math>8.9 \times 10^{-3}</math> (0.3)</b>	<b>0.71 (0.15)</b>
	<b><math>3.3 \times 10^{-2}</math> (0.6)</b>	<b>1.01 (0.3)</b>
	0.35 (2)	<b>1.43 (0.6)</b>

433 a) comonomer concentrations ratios corresponding to the calculated ratios of rates of comonomer  
434 consumption, assuming the validity of the Mayo-Lewis equation (steady state conditions), are  
435 given in parentheses (in bold data for initial ratios for analyzed copolymerizations are given).

436 Rather unexpected was the finding that the difference between **Tmc** reactivity ratios in relation  
437 to configuration of **Ini** ( $r_{T(R)} > r_{T(S)}$ ) is as large as three orders of magnitude. It stems probably from  
438 strong steric hindrance of *R*-**Ini** residue of active species while the transition state for **Lac** addition to  
439 **Tmc\*** is formed. The corresponding hindrance for **Tmc** addition is smaller because of the lack of  
440 methyl groups, present in **Lac**. On the other hand, the smaller difference observed for **Lac** reactivity  
441 ratios ( $r_{L(R)} > r_{L(S)}$ ) and indicating that addition of **Lac** to **Lac\*** is faster than addition of **Tmc** for both  
442 configurations of **Ini**, is probably due to relatively large differences in activation enthalpies of the  
443 corresponding reactions.

444 It is important to indicate here that our fitting computations could not estimate the  $Z_{LL}$   
445 parameter in copolymerizations initiated with *S-Ini*, nor initiated with the mixture of *Ini*  
446 enantiomers. It is so, because of the systems quickly attaining steady state conditions maintaining  
447 the proportion of active species. These steady state conditions, applied also while deriving  
448 Mayo-Lewis equations, are generally accepted while analyzing copolymerization kinetics. However,  
449 when at least one of reactivity ratios is very high, attaining of the steady state conditions can require  
450 quite large conversions. For such systems, here observed for *R-Ini* initiated *Lac/Tmc*  
451 copolymerization, the Mayo-Lewis equations can be regarded as giving only crude estimates for  
452 relative rates of comonomer consumptions. In fact, the  $Z_{LL}$  parameter in 'normal' copolymerizations  
453 determines the steady state condition ratio of concentrations of *Lac\** and *Tmc\** active species, not  
454 influencing the relative rates of comonomer consumption. The estimation of the  $Z_{LL} = k_{LL}/k_{TT}$   
455 parameter can be done only applying some specific methods, for instance analyzing in details the  
456 molar mass distribution in relation to chain compositions [37].

457 Thus, in our simulations, when fitting the relative kinetic parameters for *S-Ini* systems by  
458 minimization of the defined objective function (see Supporting information), we observed, as  
459 expected, independence of the fitting results for  $r_L$  and  $r_T$ , for any assumed value for  $Z_{LL}$  in the range  
460 between  $10^{-2}$  and  $10^2$  (not checked outside this range).

461 On the other hand, due to not steady state conditions up to high conversions, while fitting  
462 relative parameters for *R-Ini* systems we could attain minima of the objective function (see  
463 Supporting information), giving different results for  $r_L$  and  $r_T$ , for any assumed value of  $Z_{LL}$ . Besides,  
464 also due to slow attaining the steady state conditions, the fitting results depended on the assumed  
465 proportion of initiating unimers. The observed minima were on quite similar levels for  $Z_{LL}$  in the  
466 range between  $10^{-3}$  and 0.5, being on apparently higher levels outside this range. Thus, our estimates  
467 of the reactivity ratios  $r_L$  and  $r_T$  and of the relative rates of comonomer consumption for *R-Ini*  
468 systems, given in the Table 2, are rather crude. They were obtained for  $Z_{LL}$  equal to  $4 \cdot 10^{-3}$ , giving only  
469 slightly lower the objective function minimum than observed for different  $Z_{LL}$  in the indicated range.  
470 Moreover, these estimates were obtained assuming initiation exclusively with *Tmc* unimers. The last  
471 assumption was made because of the observed large differences of rates of homopolymerization of  
472 *Tmc* and *Lac* initiated with *R-Ini*, *Tmc* polymerizing much faster, see Supporting information.

473 The results presented in Table 2 indicate tremendous differences between copolymerization  
474 systems differing only in configuration of asymmetric bulky initiator. While *R-Ini* gives copolymer  
475 of virtually oligoblock structure: initially mostly only *Tmc* is consumed, forming the corresponding  
476 blocks, and next the blocks of poly-*Lac* are formed. The product of reactivity ratios is very high,  
477 indicating that practically negligible inserts of *Lac* units in the initial, mostly homo-*Tmc* parts of  
478 chains, are short blocks of *Lac* rather than separate single *Lac* units. Similarly, at the end parts of  
479 chains, being approximately the *Lac* homo-blocks, one can expect only infrequent inserts of short  
480 homo-blocks of *Tmc*. However, due to a very high  $r_L$ , similarly as of  $r_T$ , and  $k_{LL} \ll k_{TT}$ , ( $Z_{LL}$  estimated  
481 to be about  $10^{-2}$ ) some homo-*Lac* chains, if formed in the initial part of copolymerization, grow  
482 slower than chains formed from *Tmc* unimers. Some of these chains can survive till the end of  
483 copolymerizations, forming small, not negligible for systems with not sufficiently high  $DP_n$ ,  
484 fractions of homo *Lac* polymer, differing in the average molar mass from copolymer chains. One  
485 cannot also exclude formation of a fraction of homo-*Tmc* polymer in some copolymerization  
486 systems. This characteristics of *R-Ini* copolymerization systems results in dispersity of product  
487 significantly higher than expected for random copolymerizations proceeding without side reactions  
488 like, for instance, segmental exchange or cyclizations. Even if one assume that the system is initiated  
489 only with *Tmc* unimers (as done by us in simulations giving  $r_L$  and  $r_T$  values for *R-Ini* systems in  
490 Table 1), dispersity can be quite high, due to slow transformation of *Tmc\** chains into *Lac\** chains.  
491 This phenomenon resembles slow initiation, which also leads to broadened dispersity.

492 On the other hand, using as initiator the *S-Ini* results in initial rates of consumption of both  
493 comonomers not differing much and in some tendency to alternacy (product of reactivity ratios  
494 about 0.1). Due to the excess of *Tmc* in all studied copolymerization systems one can expect

495 copolymer chains ended with homoblocks of **Tmc** containing some small amount of inserts of  
 496 separated units of **Lac**.

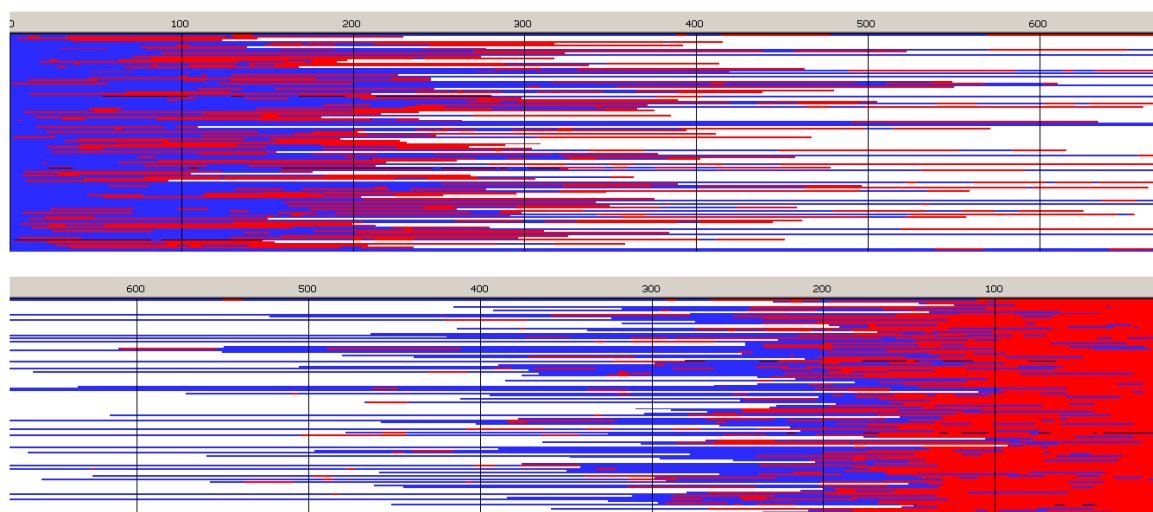
497 Our Monte Carlo simulations confirm the above description of copolymer chains, deduced  
 498 from the estimated reactivity ratios for products obtained in the studied systems.

499 However, there was one experimental inconsistency of numerical simulations with  
 500 experimental data. Namely, dispersity of copolymer chains initiated with *S*-**Ini** (fast  
 501 inter-transformations of **Lac**<sup>\*</sup> and **Tmc**<sup>\*</sup> active species), are significantly higher than expected from  
 502 simulations assuming, as mentioned above, fast exchange of active chain-ends with hydroxyl  
 503 terminated ones. A relatively large dispersity (above 1.5 for higher conversions) was successfully  
 504 explained by the rate of the exchange reactions involving OH terminated chains (Scheme 6) being  
 505 not sufficiently high. Therefore, the copolymerization systems do not behave exactly, as expected  
 506 from simulations assuming the discussed till now model. Verifying this hypothesis with Monte  
 507 Carlo simulations we came to conclusion that the hydroxyl terminated chains are probably  
 508 transformed into living chains with rates much lower than propagation, resulting in broadening of  
 509 the molar mass distribution. Numerical simulations, described in Supporting information, taking  
 510 into account the slow chain-transfer processes, allowed to estimate the average relative rate  
 511 constants of chain-exchange in analyzed copolymerizations  $k_{ex}/k_{TT}$  as well as the effective ratio of  
 512 homopropagation rate constants  $k_{LLR}/k_{LLS}$ , important for systems initiated with the mixture of **Ini**  
 513 enantiomers, described below.

514 Consequently, the presented below results take into account the chain-end exchange reactions  
 515 in all studied systems.

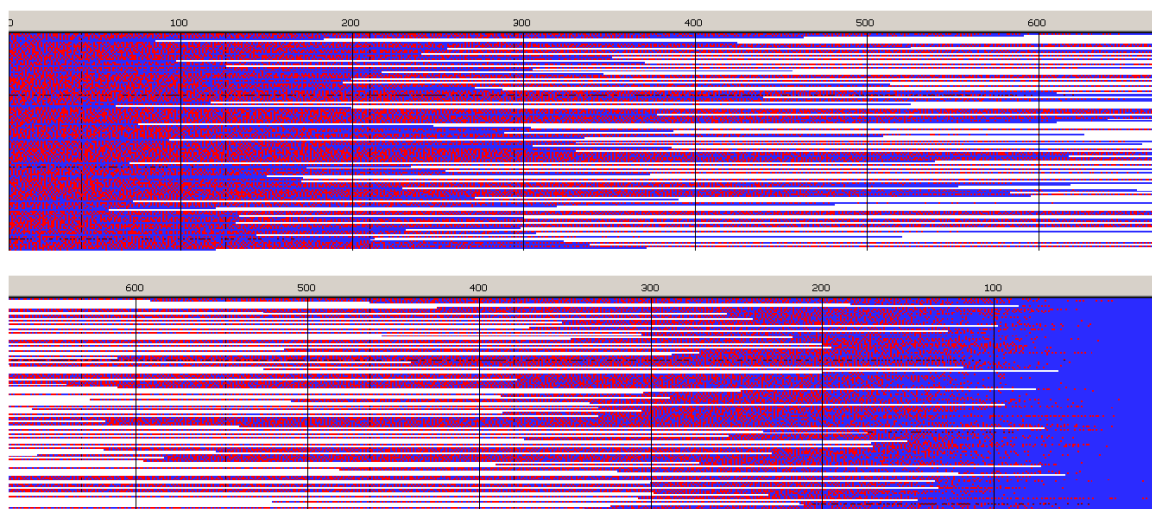
516 Figures 6-9 present structures of copolymer chains formed in systems initiated by *S*- or *R*-  
 517 enantiomer of **Ini**, simulated by MC method neglecting depropagation reactions. Initial  
 518 concentrations of reagents were the same:  $[Tmc]_0 = 2$ ,  $[Lac]_0 = 1.2 \text{ mol L}^{-1}$ , and  $[Ini]_0 = 2 \cdot 10^{-3} \text{ mol L}^{-1}$  (+  
 519  $[iPrOH]_0 = 4 \cdot 10^{-3} \text{ mol L}^{-1}$  due to *in situ* synthesis of **Ini**). The only difference consisted in initiation by  
 520 **Tmc**<sup>\*</sup> unimer in case of *R*- enantiomer and mixture of **Tmc**<sup>\*</sup> and **Lac**<sup>\*</sup> unimers (proportionally to  
 521 comonomer concentrations) in case of *S*-enantiomer. Reactivity ratios used in each simulation are  
 522 given in Table 2. Top boxes: plots prepared using unit positions numerated starting from chain  
 523 beginning, bottom boxes: starting units numeration from chain-end.  
 524

525



526

527 **Figure 6.** Sample of simulated chains in copolymerization initiated with **Tmc-R-Ini**<sup>\*</sup>. Reactivity ratios  
 528 as given in Table 2,  $Z_{LL} = 3.8 \cdot 10^{-3}$ ,  $k_{ex}/k_{TT} = 4 \cdot 10^{-2}$ .  $[Tmc]_0 = 2$ ,  $[Lac]_0 = 1.2 \text{ mol L}^{-1}$ , and  $[Ini]_0 = 2 \cdot 10^{-3} \text{ mol}$   
 529  $\text{L}^{-1}$  (+  $[iPrOH]_0 = 4 \cdot 10^{-3} \text{ mol L}^{-1}$  due to *in situ* synthesis of **Ini**). Conversion 95%,  $DP_n = 507.4$ ,  $D = 1.48$ ,  
 530 average number of homoblocks per chain equal to 5.2. Red and blue mark **Lac** and **Tmc** units,  
 531 respectively. Top box: unit positions numerated starting from chain beginning, bottom box: starting  
 532 from chain-end. For the sake of plots clarity the chains longer than  $DP = 1.3 DP_n$  are shown only  
 533 partially (this applies also to similar plots below).



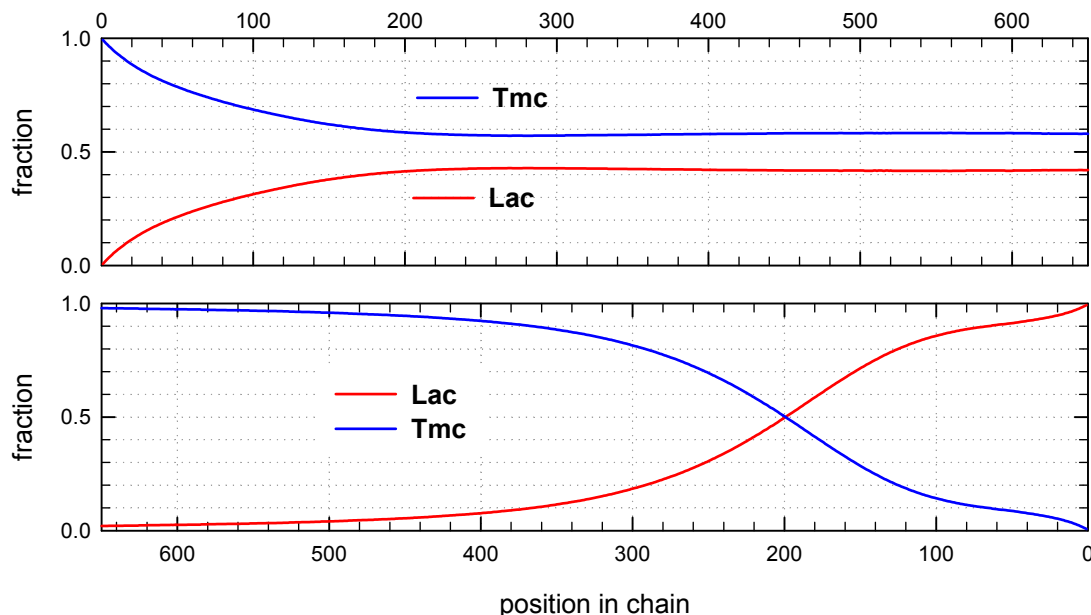
534

535

536 **Figure 7.** Sample of simulated chains in copolymerization initiated with **S-Ini** (mixture of **Lac\*** and  
 537 **Tmc\*** unimers). Reactivity ratios  $Z_{LL} = 37.6$ ,  $k_{ex}/k_{TT} = 8.1$ . Other conditions as in Figure 6. Conversion  
 538 95%,  $DP_n = 506.4$ ,  $D = 1.40$ , average number of homoblocks in a chain equal to 292.

539 Copolymer formed with **R-Ini** and initiated with **Tmc\*** unimers (Figure 6) is a block copolymer,  
 540 containing on the average 5.2 blocks in a chain. As it was initiated with **Tmc** unimers chains start  
 541 with **Tmc** blocks and, due to faster consumption of **Tmc**, chains are terminated with **Lac** blocks.

542 Monte Carlo simulations allow to present also the average composition of copolymers along  
 543 average chain (computed for the whole set of chains) as well as similar distribution of homo and  
 544 hetero dyads. The corresponding plots are shown in Figures 8-9.



545

546 **Figure 8.** Distribution of copolymer units along an average chain expressed as mole fractions for  
 547 system initiated with **Tmc-R-Ini\*** unimer. The relative kinetic parameters as shown in Table 2 and  
 548 caption to Figure 6. Unit positions numerated from chain beginning (top box) and from the  
 549 chain-end (bottom box).

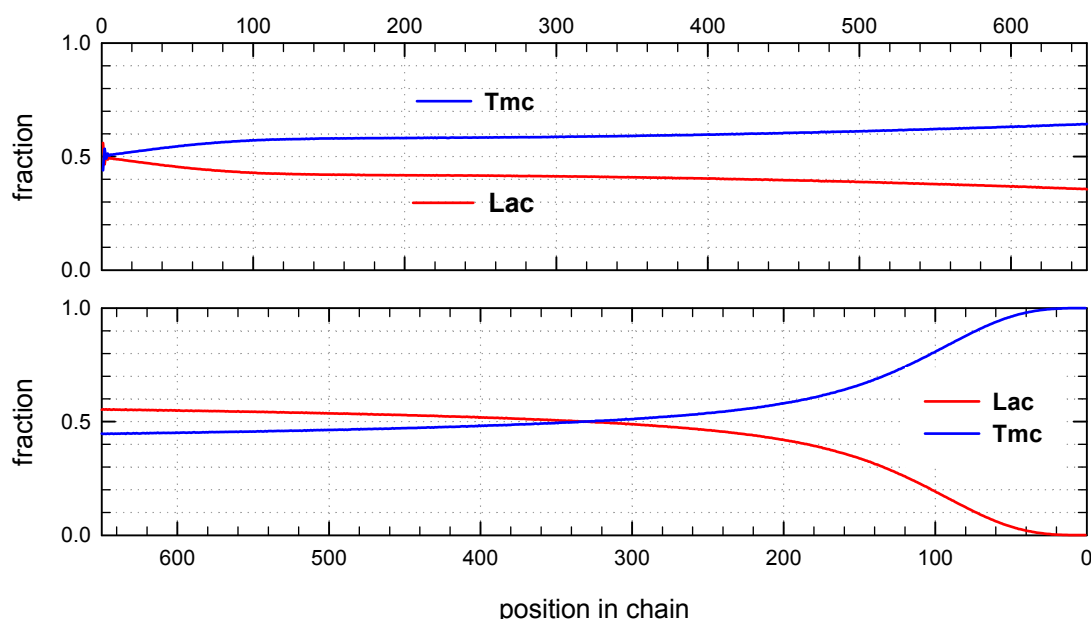
550 The corresponding plots differ, being dependent on numeration of unit positions, starting  
 551 either from the chain beginning or chain-end. Due to rather broad molar mass distribution these  
 552 differences are quite large. If position of unit is counted from chain beginning the fractions of  
 553 copolymer units at more distant positions come to plateau and practically does not change up to



554 chain positions at least about twice  $DP_n$ . On the other hand, if unit positions are counted from  
 555 chain-ends, one can clearly see gradient-like feature of copolymer chains.

556 Distribution of units in copolymer formed with *S-Ini* and initiated with the mixture of  
 557 **Lac-S-Ini\*** and **Tmc-S-Ini\*** unimers, in proportion corresponding to initial concentration of  
 558 comonomers (1.2:2) (Figure 7) differs significantly from system initiated by **Tmc-R-Ini\*** unimers.

559 Initial parts of chains, exceeding up to about 70% of chain length, contain statistical distribution  
 560 of comonomers, apparently with close to each other proportion of comonomer units, no gradient of  
 561 comonomer composition along individual chains in these regions visible. However, when we  
 562 analyze positions of units and sequences in the whole set of copolymer chains, the contributions of  
 563 **Lac** and **Tmc** units (Figure 9) change slightly steadily with unit position, indicating gradient feature.  
 564 The shapes of the corresponding plots differ, depending on that if unit positions are numerated  
 565 starting from the chain beginning or chain-end, similarly as it was observed for *R-Ini* system.



566

567 **Figure 9.** Distribution of copolymer units along an average chain expressed as mole fractions for  
 568 system initiated with the mixture of **Lac-S-Ini\*** and **Tmc-S-Ini\*** unimers. The relative kinetic  
 569 parameters as shown in Table 2 and caption to Figure 7. Unit positions numerated from chain  
 570 beginning (top box) and from the chain-end (bottom box).

571 In the Supporting information one can find the similar plots presenting distribution of dyads  
 572 and the average lengths of homoblocks along chain for systems initiated with both **Ini** enantiomers.

573 The presented copolymer structures Figures 6 and 7 were prepared choosing the exchange  
 574 relative parameter  $z_{ex}$  (listed in the Figure captions) to get dispersity close to the observed in  
 575 experiments. One can observe that  $z_{ex}$  for *R-* and *S-Ini* systems differ significantly. It stems probably  
 576 not only from different reactivities of **Lac-R-Res\*** and **Lac-S-Res\*** species (diastereomers) but also  
 577 from the simplifying assumption (see Supporting information) that all relative kinetic exchange  
 578 parameters are equal, independently on copolymer units neighboring OH group or *R/S-Ini* residue  
 579 of active centers.

580 The rate of chain-end exchange is more important in copolymerization system initiated with the  
 581 mixture of *R* and *S* enantiomers of **Ini**. It is so because beside determining copolymer dispersity it  
 582 predetermines also the effective rate of exchange of the **Ini** residues of different configuration at  
 583 active chain-ends and consequently the chain reactivity ratios, establishing copolymer  
 584 microstructure. Any growing chain can, if the exchange is sufficiently fast, change configuration of  
 585 its active species, with frequency dependent on the discussed relative rate coefficient  $z_{ex}$ .

586 3.3. Copolymerization initiated with the mixture of enantiomers of **Ini**

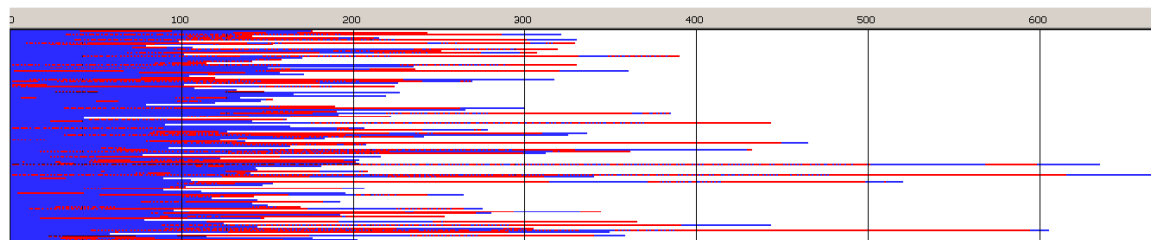
587 The observed differences in features of copolymerization systems initiated with *R-Ini* and *S-Ini*  
588 suggests that one can control to some extent copolymerization features by using instead of one  
589 enantiomer of the studied asymmetric bulky initiator **Ini** the mixture of its enantiomers in variable  
590 proportions.

591 We performed such an experiment choosing the proportion of initiators *R-Ini*:*S-Ini* equal to  
592 94:6. The large excess of *R* enantiomer was adopted because the rate of copolymerization initiated  
593 with *R-Ini*, leading to long homo-blocks, is much lower than that initiated with *S-Ini* and, on the  
594 other hand, the latter leads to statistical, almost alternating structures. Thus, the *S* enantiomer,  
595 although being in minority but with relatively fast cross-propagation rate constants, can effectively  
596 change the type of active species from **Lac\*** to **Tmc\*** and *vice versa*. The expected result was to obtain  
597 relatively homogeneous multi-block chains.

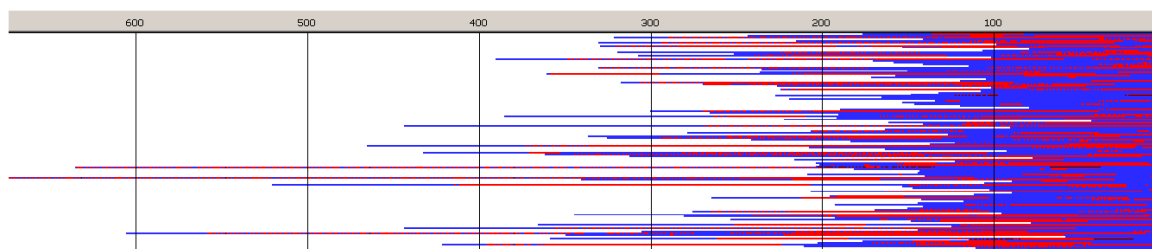
598 Copolymerization results were only partly as expected. Although the copolymerization rate  
599 and proportion of hetero-dyads were higher than in *R-Ini* copolymerization (for  $^{13}\text{C}$  NMR see the  
600 supporting information) and the average number of copolymer blocks increased, gradient-like  
601 feature is still visible in Monte Carlo simulations. It was explained by rather slow, not sufficiently  
602 fast, as we expected, exchange of **Lac-*R-Res\**** active species (characterized by high reactivity ratio)  
603 into **Lac-*S-Res\**** active species (via **Lac-OH** terminating chains, acting as intermediates). If this  
604 process was fast enough, **Lac-*S-Res\**** could fast attach **Tmc** comonomer (low reactivity ratio),  
605 forming **Tmc-*S-Res\**** terminated chain, which can readily attach **Lac**. Similarly, **Tmc-*R-Res\**** active  
606 species (high reactivity ratio, slow addition of **Lac** comonomer unit), apparently not so fast as we  
607 expected, can be transformed (also via OH terminated intermediate) into **Tmc-*S-Res\**** attaching next  
608 relatively quickly **Lac**, forming **Lac-*S-Res\**** species, already discussed. Consequently, contribution of  
609 heterodyads, as observed in  $^{13}\text{C}$  NMR spectrum (Supporting information), is higher than in  
610 copolymer formed with *R-Ini*, but instead of approximately homogeneous unit distribution, one can  
611 rather expect regions in one chain differing in microstructure: those formed with *R-Ini\** and ones  
612 formed with *S-Ini\** active species

613 Monte Carlo simulations, presented in Figures 10-11 (and those in Supporting information)  
614 confirm the described briefly structure of copolymer. The average number of blocks is significantly  
615 higher (25.3) than estimated for copolymerization initiated with *R-Ini* (5.2). Unfortunately, due to  
616 not sufficiently fast exchange of *R* and *S* active species one can easily find (Figure 10) segments of  
617 copolymer chains containing statistical distribution of copolymer chains. Consequently, dispersity  
618 of block-lengths is high at any chain position (see Supporting information), being the highest at the  
619 beginning of chains (about 10 for **Lac**, and about 16 for **Tmc** blocks) and the lowest at chain positions  
620 close to active species (about 4-5 for both types of blocks). In the Supporting information one can  
621 find also the plots presenting the computed distribution of dyads and the average lengths of  
622 homoblocks along chain and the discussion concerning the average homoblock lengths along  
623 copolymer chains. The average homoblock lengths can be calculated not only in dependence on  
624 chain position, but also on the way the homoblocks are selected for computing their average *DP*.

625



626



627

628

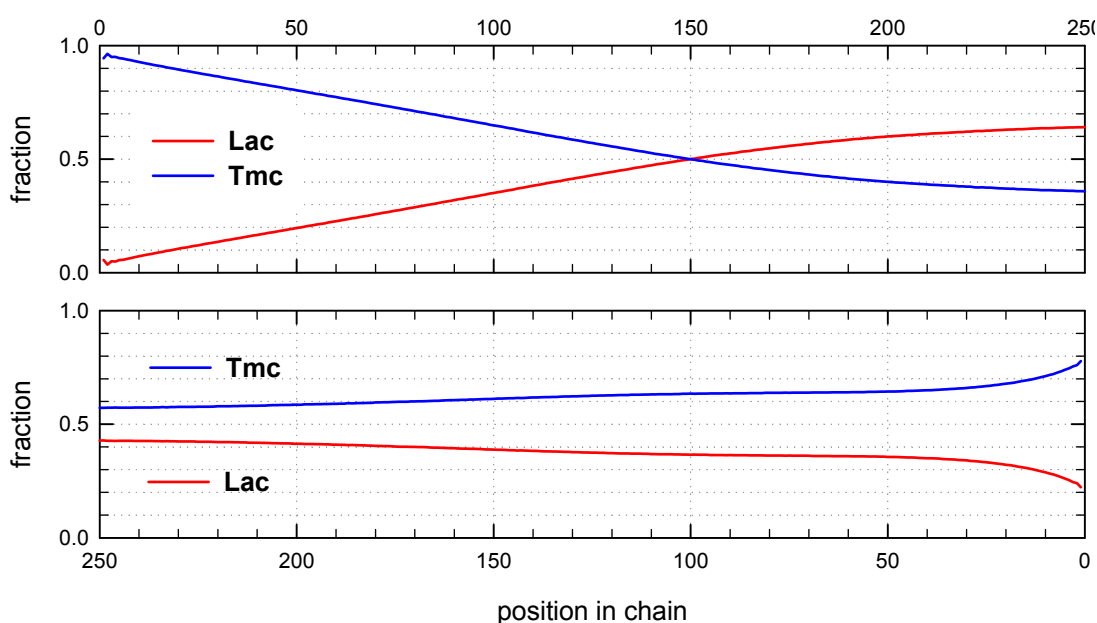
629

630

631

632

**Figure 10.** Sets of simulated copolymer chains in copolymerization initiated with the mixture of *R*- and *S*-**Ini** (94:6). Reactivity ratios as given in Table 2,  $Z_{LLR} = 6.92$ ,  $Z_{LLS} = 1.45$ , and the ratio of **Tmc** homopropagation rate constants,  $k_{TTR}/k_{TTS}$ , being about 0.78.  $[Tmc]_0 = 2$ ,  $[Lac]_0 = 1.2 \text{ mol L}^{-1}$ , and  $[Ini]_0 = 5 \cdot 10^{-3}$  (+  $[iPrOH]_0 = 1 \cdot 10^{-2}$ , due to *in situ* synthesis of **Ini**), Conversion 95%,  $DP_n = 202.1$ ,  $D = 1.27$ , average number of homoblocks in a chain equal to 25.2.



633

634

635

**Figure 11.** Distribution of copolymer units along chain for conditions given in Figure 10. Chain positions numerated from chain beginning (top) and from active center (bottom).

636

637

638

639

640

641

642

643

644

645

646

647

648

649

650

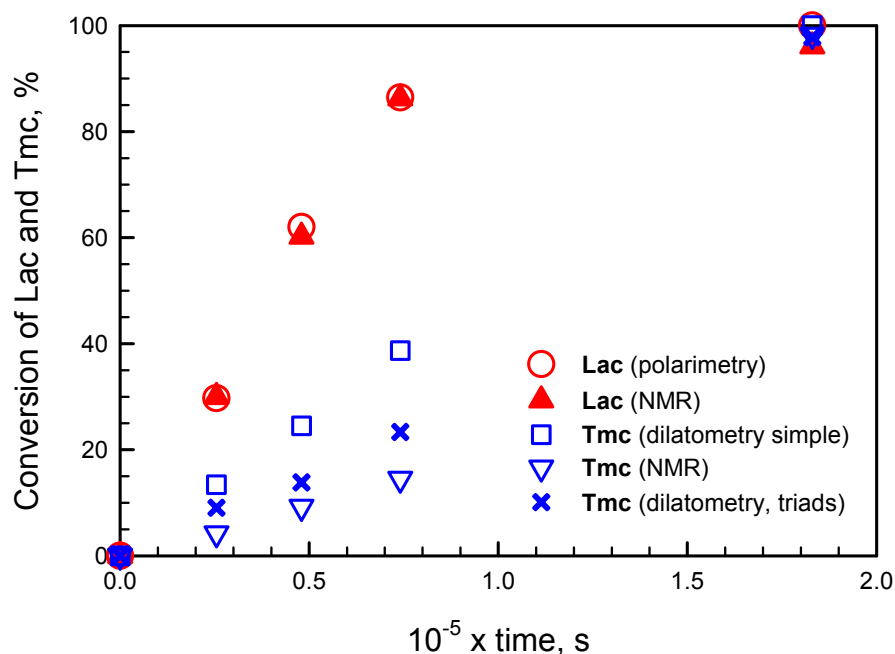
651

652

653

Analyzing this copolymerization and performing fitting computations we got to rather unexpected result. Namely, the reasonably good fitting of kinetic parameters for the chain-end *R/S* exchanging systems was achieved only when we have removed restriction of equal **Tmc** homopropagation rate constants on active species terminated with initiator residue **Res** of different configuration. It can be explained by solvation of **Tmc-Res\*** active species (of both **Ini** configurations) by asymmetric **Lac** comonomer molecules and corresponding copolymer units. Depending on configuration of **Res** presumably different average numbers of asymmetric **Lac** monomers/copolymer units solvate active species, and consequently also different numbers of **Tmc** molecules can be present in the corresponding solvation spheres. Thus, different spatial molecular arrangements can be expected around **Tmc-R-Res\*** and **Tmc-S-Res\*** active species. In fact, taking into account asymmetric solvating entities one can consider these active species with their solvation spheres as different environments or arrangements, what results in their different reactivities, and consequently different **Tmc** homopropagation rate constants  $k_{TTR} \neq k_{TTS}$ . These differences in solvation spheres can be of two kinds: **Tmc-R-Res\***(solvated) and **Tmc-S-Res\***(solvated) can be diastereomeric if the same numbers of **Lac** monomer molecules and copolymer units are present in them, or they can differ in numbers of **Tmc** molecules if enantiomeric **Tmc-Res\*** active species differ in accepting in their solvation spheres asymmetric **Lac** molecules, competing with symmetric **Tmc** molecules.

654 We believe that this presumption based on our simulations (that  $k_{TTR} \neq k_{TTS}$ ) is sound because  
 655 not only the corresponding fitting to experimental [Lac] and  $\Delta H$  is the best but also it gives the  
 656 closest agreement with experimental [Tmc], determined with  $^{13}\text{C}$  NMR (Figure 12).  
 657



658

659 **Figure 12.** Evolution of **Lac** and **Tmc** conversions in system initiated by mixture of *R*- and *S*-**Ini**  
 660 (conditions given in Figure 10) determined by  $^{13}\text{C}$  NMR, polarimetry, and two dilatometric methods:  
 661 a simple (assuming equal volume contraction coefficients) and devised by us taking into account  
 662 triad dependence of CC (and assuming  $\text{CC}_{TTL} + \text{CC}_{LTT} = \text{CC}_{TTT} + \text{CC}_{LTL}$ , as well as  $k_{TTR} \neq k_{TTS}$ ).

663 Although this correlation between  $[\text{Tmc}]_{\text{exp}}$  and  $[\text{Tmc}]_{\text{calc}}$  obtained applying the devised method  
 664 with triad dependence of volume contraction coefficients CC is not very good, we think that the  
 665 observed differences stem from our approximations concerning the assumed model of  
 666 copolymerization. Namely, the assumed very similar, parallel changes of rate coefficients with  
 667 conversion and also the approximations concerning volume contraction coefficients may be  
 668 responsible for the observed discrepancy. We think that the largest errors in estimation of **Tmc**  
 669 concentrations are introduced by the limitation of the number of CC coefficients to be fitted, done by  
 670 assumption that  $\text{CC}_{AAB} + \text{CC}_{BAA} = \text{CC}_{AAA} + \text{CC}_{BAB}$  (see Supporting information).

#### 671 4. Conclusions

672 We have shown that a bulky asymmetric initiator 2,2'-[1,1'-binaphthyl-2,2'-diyl-bis-  
 673 (nitrylometilidyne)]diphenoxy aluminum isopropoxide used in copolymerization of asymmetric  
 674 monomer **Lac** with symmetric comonomer **Tmc** gives an opportunity of synthesis of product of a  
 675 range of possible structures. Copolymer structure can be controlled by the choice of the initiator  
 676 enantiomer, or proportion of both used simultaneously, as well as by the proportion of initial  
 677 comonomer concentrations. When *R* enantiomer is used a copolymer built of long homoblocks is  
 678 formed. Moreover, it can contain some fractions of homo-**Lac** and homo-**Tmc** polymers. On the other  
 679 hand, using the *S*-**Ini** results in a statistical copolymer containing random fragments with some  
 680 tendency to alternacy at the beginning of chains, with approximately 1:1 distribution of copolymer  
 681 units and homoblocks of **Tmc** at the end of chains (if, as in our experiments, this comonomer is used  
 682 in excess).

683 When copolymerization is initiated with the mixture of *R*-**Ini** and *S*-**Ini** then copolymer of some  
 684 intermediate structure can be obtained. For instance using the 94:6 proportion of initiator  
 685 enantiomers one can obtain a multiblock copolymer with blocks much shorter than those formed  
 686 while using *R* enantiomer.

687 Another important result of our investigation is a rather general observation that analysis of  
688 dilatometric data for copolymers may require, as it was in our systems, taking into account the  
689 different volume contraction coefficients for copolymer units in different triads. We have proposed  
690 the way of solving this analytical problem by numerical fitting of the simulated copolymerization  
691 kinetics to experimental data.

692 The analysis of copolymerization kinetics suggests that kinetic rate coefficients in our systems  
693 change with conversion, what was explained by variation of solvation effect involving asymmetric  
694 comonomer molecules and copolymer units. This solvation effect can also explain the difference of  
695 rate coefficients of **Tmc** homopropagation on *R* and *S* enantiomeric **Tmc**\* active species.

696 **Supplementary Materials:** The following are available online at [www.mdpi.com/link](http://www.mdpi.com/link), PDF document  
697 containing additional spectra, plots, and equations, not included in the main text.

698 **Acknowledgments:** This study was supported by project “Biodegradable fibrous products” (BIOGRATEX),  
699 realized upon Contract Number POIG.01.03.01-00-007-/08-00 and co-financed by European Union. Numerical  
700 simulations and corresponding analysis were supported by the National Science Center, Poland, Grant No.  
701 DEC-2014/15/B/ST5/05321. Authors thank Prof. M. Cypryk for the valuable discussion during preparation of  
702 this paper.

703 **Author Contributions:** Marta Socka and Andrzej Duda conceived and designed the experiments; Marta Socka  
704 performed experiments and instrumental analyses; Marta Socka, Ryszard Szymanski, and Stanislaw  
705 Sosnowski analyzed the data, Stanislaw Sosnowski and Ryszard Szymanski contributed simulation software  
706 and performed numerical simulations; Marta Socka and Ryszard Szymanski wrote the paper with support of  
707 Stanislaw Sosnowski.

708 **Conflicts of Interest:** The authors declare no conflict of interest.

## 709 References

- 710 1. *Biomaterials for Tissue Engineering Applications*; Burdick J.A., Mauck R.L., Eds.; Springer Verlag, New York,  
711 USA 2011; ISBN 978-370-910-384-5.
- 712 2. *Polymers in Drug Delivery*; Uchegbu I., Schatzlein A.G., Eds; CRC Press: Boca Raton, USA, 2006; ISBN  
713 978-084-932-533-5. *Handbook of Polyester Drug Delivery Systems*; Ravi Kumar, M.N.V. Ed.; Pan Stanford:  
714 Singapore, 2016; ISBN 978-981-466-965-8.
- 715 3. Zhang, Z.; Grijpma, D.W.; Feijen, J. Triblock copolymers based on 1,3-trimethylene carbonate and lactide  
716 as biodegradable thermoplastic elastomers. *J. Macromol. Chem. Phys.* **2004**, *205*, 867–875, doi:  
717 10.1002/macp.200300184.
- 718 4. Guerin, W.; Helou, M.; Carpentier, J.-F.; Slawinski, M.; Brusson, J.-M.; Guillaume, S.M. Macromolecular  
719 engineering via ring-opening polymerization (1): L-lactide/trimethylene carbonate block copolymers as  
720 thermoplastic elastomers. *Polym. Chem.* **2013**, *4*, 1095–1106, doi: 10.1039/c2py20859h.
- 721 5. Guerin, W.; Helou, M.; Slawinski, M.; Brusson, J.-M.; Guillaume, S.M.; Carpentier, J.-F. Macromolecular  
722 engineering via ring-opening polymerization (2): L-lactide/trimethylene carbonate copolymerization -  
723 kinetic and microstructural control via catalytic tuning. *Polym. Chem.* **2013**, *4*, 3686–3693, doi:  
724 10.1039/c3py00397c.
- 725 6. Pêgo, A.P.; van Luyn, M.J.A.; Brouwer, L.A.; van Wachem, P.B.; Poot, A.A.; Grijpma, D.W.; Feijen, J. In  
726 vivo behavior of poly(1,3-trimethylene carbonate) and copolymers of 1,3-trimethylene carbonate with  
727 D,L-lactide or epsilon-caprolactone: Degradation and tissue response. *J. Biomed. Mater. Res.* **2003**, *67A*,  
728 1044–1054, doi: 10.1002/jbm.a.10121.
- 729 7. Duda, A. ROP of Cyclic Esters. Mechanisms of Ionic and Coordination Processes. In *Polymer Science: A*  
730 *Comprehensive Reference*; Matyjaszewski, K., Möller, M., Eds.; Elsevier BV: Amsterdam, Holland, 2012; vol.  
731 4, pp. 213–246, ISBN 978-044-453-349-4.
- 732 8. Duda, A.; Kowalski A. Thermodynamics and Kinetics of Ring - Opening Polymerization. In *Handbook of*  
733 *Ring-Opening Polymerization*, Dubois, P., Coulembier, O., Raquez, J.-M., Eds.; Wiley-VCH Verlag GmbH &  
734 Co. KGaA: Weinheim, Germany, 2009; chap. 1, pp. 1–51, ISBN 978-352-731-953-4.
- 735 9. Slomkowski, S.; Penczek, S.; Duda, A. Polylactides-an overview. *Polym. Adv. Technol.* **2014**, *25*, 436–447,  
736 doi: 10.1002/pat.3281.

- 737 10. Rokicki, G.; Parzuchowski, P.G. ROP of Cyclic Carbonates and ROP of Macrocycles. In *Polymer Science: A*  
738 *Comprehensive Reference*; Matyjaszewski, K., Möller, M., Eds.; Elsevier BV: Amsterdam, Holland, 2012; vol.  
739 4, pp. 247–303, ISBN 978-044-453-349-4.
- 740 11. Kowalski, A.; Libiszowski, J.; Duda, A.; Penczek, S. Polymerization of L,L-dilactide initiated by tin(II)  
741 butoxide. *Macromolecules* **2000**, *33*, 1964–1971, doi: 10.1021/ma991751s.
- 742 12. Jarrett, P.K.; Casey, D.J. Deformable, absorbable surgical device. U.S. Patent 5376102 A, 1994.
- 743 13. Roby, M.S.; Kokish, L.K.; Mehta, R.M.; Jomn, J.Y. Absorbable polymers and surgical articles fabricated  
744 therefrom. U.S. Patent 6235869 B1, 2001.
- 745 14. Ruckenstein, R.; Yuan, Y. Molten ring-open copolymerization of L-lactide and cyclic trimethylene  
746 carbonate. *J. Polym. Sci. Part A: Polym. Chem.* **1998**, *69*, 1429–1434, doi:  
747 10.1002/(SICI)1097-4628(19980815)69:7<1429::AID-APP18>3.0.CO;2-O.
- 748 15. Cai, J.; Zhu, K.J. Preparation, Characterization and Biodegradable Characteristics of Poly(D,L-lactide-co-  
749 1,3-trimethylene carbonate). *Polym. Int.* **1997**, *42*, 373–379, doi: 10.1016/S0032-3861(97)10346-9.
- 750 16. Cai, J.; Zhu, K.J.; Yang, S.L. Surface biodegradable copolymers—poly(d,l-lactide-co-1-methyl-  
751 1,3-trimethylene carbonate) and poly(d,l-lactide-co-2,2-dimethyl-1,3-trimethylene carbonate): preparation,  
752 characterization and biodegradation characteristics in vivo. *Polymer* **1998**, *39*, 4409–4415, doi:  
753 10.1016/S0032-3861(97)10346-9.
- 754 17. Pêgo, A.P.; Poot, A.A.; Grijpma, D.W.; Feijen, J. *Macromol. Biosci.* **2002**, *2*, 411–419, doi:  
755 10.1002/mabi.200290000.
- 756 18. Pospiech, D.; Komber, H.; Jehnichen, D.; Häussler, L.; Eckstein, K.; Scheibner, H.; Janke, A.; Kricheldorf,  
757 H.R.; Petermann, O. Multiblock copolymers of L-lactide and trimethylene carbonate. *Biomacromolecules*  
758 **2005**, *6*, 439–446, doi: 10.1021/bm049393a.
- 759 19. Yang, J.; Yu, Y.H.; Li, Q.B.; Li, Y.; Cao, A.I. Chemical synthesis of biodegradable aliphatic polyesters and  
760 polycarbonates catalyzed by novel versatile aluminum metal complexes bearing salen ligands. *J. Polym.*  
761 *Sci. Part A: Polym. Chem.* **2005**, *43*, 373–384, doi: 10.1002/pola.20507.
- 762 20. Zhou, L.; Sun, H.; Chen, J.; Yao, Y.; Shen, Q. Homoleptic lanthanide guanidinate complexes: The effective  
763 initiators for the polymerization of trimethylene carbonate and its copolymerization with  $\epsilon$ -caprolactone.  
764 *J. Polym. Sci. Part A: Polym. Chem.* **2005**, *43*, 1778–1786, doi: 10.1002/pola.20644.
- 765 21. Nakayama, Y.; Yasuda, H.; Yamamoto, K.; Tsutsumi, C.; Jerome, R.; Lecompte, P. Comparison of Sm  
766 complexes with Sn compounds for syntheses of copolymers composed of lactide and cyclic carbonates and  
767 their biodegradabilities. *React. Funct. Polym.* **2005**, *63*, 95–105, doi: 10.1016/j.reactfunctpolym.2005.02.012.
- 768 22. Agarwal, S.; Puchner, M.; Greiner, A.; Wendorff, J.H. Synthesis and microstructural characterisation of  
769 copolymers of L-lactide and trimethylene carbonate prepared using the SmI<sub>2</sub>/Sm initiator system. *Polym.*  
770 *Int.* **2005**, *54*, 1422–1428, doi: 10.1002/pi.1865.
- 771 23. Dobrzynski, P.; Kasperczyk, J. Synthesis of biodegradable copolymers with low-toxicity zirconium  
772 compounds. V. Multiblock and random copolymers of L-lactide with trimethylene carbonate obtained in  
773 copolymerizations initiated with zirconium(IV) acetylacetonate. *J. Polym. Sci.: Part A: Polym. Chem.* **2006**,  
774 *44*, 3184–3201, doi: 10.1002/pola.21428.
- 775 24. Simic, V.; Pensec, S.; Spassky, N. Synthesis and characterization of some block copolymers of lactides with  
776 cyclic monomers using yttrium alkoxide as initiator. *Macromol. Symp.* **2000**, *153*, 109–121, doi:  
777 10.1002/1521-3900(200003)153:1<109::Aid-Masy109>3.0.Co;2-5.
- 778 25. Darensbourg, D.J.; Choi, W.; Karroonnirun, O.; Bhuvanesh, N. Ring-opening polymerization of cyclic  
779 monomers by complexes derived from biocompatible metals. Production of poly(lactide),  
780 poly(trimethylene carbonate), and their copolymers. *Macromolecules* **2008**, *41*, 3493–3502, doi:  
781 10.1021/ma800078t.
- 782 26. Tsutsumi, C.; Nakagawa, K.; Shirahama, H.; Yasuda, H. Biodegradations of statistical copolymers  
783 composed of D,L-lactide and cyclic carbonates. *Polym. Int.* **2003**, *52*, 439–447, doi: 10.1002/pi.1108.
- 784 27. Spassky, N.; Wisniewski, M.; Pluta, C.; LeBorgne, A. Highly stereoelective polymerization of  
785 rac-(D,L)-lactide with a chiral Schiff's base/aluminium alkoxide initiator. *Macromol. Chem. Phys.* **1996**, *197*,  
786 2627–2637, doi: 10.1002/macp.1996.021970902.
- 787 28. Socka, M.; Duda, A.; Adamus, A.; Wach, R.A.; Ulanski, P. Lactide/trimethylene carbonate triblock  
788 copolymers: Controlled sequential polymerization and properties. *Polymer* **2016**, *87*, 50–63, doi:  
789 10.1016/j.polymer.2016.01.059.

- 790 29. Radano, C.P.; Baker, G.L.; Smith, M.R. Stereoselective polymerization of a racemic monomer with a  
791 racemic catalyst: Direct preparation of the polylactic acid stereocomplex from racemic lactide. *J. Am. Chem.*  
792 *Soc.* **2000**, *122*, 1552–1553, doi: 10.1021/ja9930519.
- 793 30. Ovitt, T.M.; Coates, G.W.; Stereoselective ring-opening polymerization of rac-lactide with a single-site,  
794 racemic aluminum alkoxide catalyst: Synthesis of stereoblock poly(lactic acid). *J. Polym. Sci. Part A: Polym.*  
795 *Chem.* **2000**, *38*, 4686–4692, doi: 10.1002/1099-0518(200012)38:1+<4686::Aid-Pola80>3.0.Co;2-0.
- 796 31. Zhong, Z.; Dijkstra, P.J.; Feijen, J. Controlled and stereoselective polymerization of lactide: Kinetics,  
797 selectivity, and microstructures. *J. Am. Chem. Soc.* **2003**, *125*, 11291–11298, doi: 10.1021/ja0347585.
- 798 32. Florczak, M.; Duda, A. Effect of the Configuration of the Active Center on Comonomer Reactivities: The  
799 Case of  $\epsilon$ -Caprolactone/L,L-Lactide Copolymerization. *Angew. Chem. Int. Ed.* **2008**, *47*, 9088–9091, doi:  
800 10.1002/anie.200803540.
- 801 33. Majerska, K.; Duda, A. Stereocontrolled polymerization of racemic lactide with chiral initiator:  
802 Combining stereoselection and chiral ligand-exchange mechanism. *J. Am. Chem. Soc.* **2004**, *126*, 1026–1027,  
803 doi: 10.1021/ja0388966.
- 804 34. Bernardo, K.D.S.; Robert, A.; Dahan, F.; Meunier, B. Preparation of New Chiral Schiff-Base Ligands  
805 Containing a Binaphthyl Moiety - X-Ray Structure of the H(2)Cl(4)Salbinapht Ligand. *New J. Chem.* **1995**,  
806 *19*, 129–131.
- 807 35. Gillespie, D.T. Exact stochastic simulation of coupled chemical reactions. *J. Phys. Chem.* **1977**, *81*, 2340–2361,  
808 doi: 10.1021/j100540a008.
- 809 36. Szymanski, R.; Sosnowski, S.; Cypriak, M. Evolution of Chain Microstructure and Kinetics of Reaching  
810 Equilibrium in Living Reversible Copolymerization. *Macromol. Theory Simul.* **2016**, *25*, 196–214, doi:  
811 10.1002/mats.201500047.
- 812 37. Szymanski, R. On the determination of the ratios of the propagation rate constants on the basis of the  
813 MWD of copolymer chains: A new Monte Carlo algorithm. *e-Polymers* **2009**, no. 044.